Open Ceramics 8 (2021) 100191

Contents lists available at ScienceDirect

Open Ceramics

journal homepage: www.sciencedirect.com/journal/open-ceramics

Literature review: Methods for achieving high powder bed densities in ceramic powder bed based additive manufacturing

Sarah Diener [a,*], Andrea Zocca [b], Jens Günster [b]

[a] Kyocera Fineceramics Precision GmbH, Lorenz-Hutschenreuther Str. 81, 95100, Selb, Germany
[b] BAM Federal Institute for Materials Research and Testing, Division 5.4 Ceramic Processing and Biomaterials, Unter Den Eichen 44 – 46, D-12203, Berlin, Germany

ARTICLE INFO

Keywords:
Powder-based process
Additive manufacturing
Powder bed density

ABSTRACT

In additive manufacturing the powder bed based processes binder jetting and powder bed fusion are increasingly used also for the production of ceramics. Final part properties depend to a high percentage on the powder bed density. Therefore, the aim is to use the best combination of powder deposition method and powder which leads to a high packing of the particles. The influence of flowability, powder properties and deposition process on the powder bed density is discussed and the different deposition processes including slurry-based ones are reviewed. It turns out that powder bed density reached by slurry-based layer deposition exceeds conventional powder deposition, however, layer drying and depowdering are extra steps or more time-consuming for the slurry route. Depending on the material properties needed the most suitable process for the part has to be selected.

1. Additive manufacturing for ceramics

Additive manufacturing (AM) is gaining more and more importance in part production in ceramic industries. There are now several providers for additively manufactured ceramic parts and printers for AM production [1].

1.1. Definition and overview of AM technologies

AM is defined as process of "joining materials to make objects from 3D model data, usually layer upon layer, as opposed to subtractive manufacturing methodologies" according to ASTM 52900 [2]. Part production starts from a CAD model which is modified for printability or oriented in such a way that e.g. no or less supports are needed or printing time is reduced due to reduced height of the build volume, then sliced and converted to a data type that the machine can work with. In the next step the 3D printing machine builds up the part according to the model. After printing the part can be removed and necessary post-processing steps such as debinding and sintering can follow before the part is used in the foreseen application.

The ASTM norm 52900 clusters AM into seven groups which are shown in Fig. 1 [2].

The seven groups of the ASTM 52900 are defined as follows [2]:

- Binder jetting: process in which a liquid bonding agent is selectively deposited to join powder materials
- Directed energy deposition: focused thermal energy is used to fuse materials by melting as they are being deposited
- Material extrusion: material is selectively dispensed through a nozzle or orifice
- Material jetting: droplets of build material are selectively deposited
- Powder bed fusion: thermal energy selectively fuses regions of a powder bed
- Sheet lamination: an AM process in which sheets of material are bonded to form an object
- Vat photopolymerization: liquid polymer in a vat is selectively cured by light-activated polymerization

There are also other classifications of AM such as dividing the methods based on their feedstock in slurry-based and powder-based methods [3]. Zocca et al. used the classes direct AM including inkjet printing and filament extrusion 3D printing and indirect AM including powder-based 3D printing, powder-based selective laser sintering, ste reolithography, slurry-based 3DP, slurry-based SLS and laminated object manufacturing [4].

AM was implemented faster for polymers and metals than for ceramics since at the beginning of AM for ceramics properties, resolution and surface quality of printed parts were not comparable to ceramics parts

* Corresponding author. Kyocera Fineceramics Precision GmbH, Lorenz-Hutschenreuther Str. 81, 95100, Selb Germany.
E-mail address: Sarah.Diener@kyocera-precision.com (S. Diener).

https://doi.org/10.1016/j.oceram.2021.100191
Received 13 August 2021; Accepted 24 September 2021
Available online 27 September 2021

which were conventionally manufactured [5]. First potential was seen for single part or low-volume productions. In traditional manufacturing complex parts often require special tools and/or long machining time where AM can be a time and cost saver or even enabler of producing a part at all [6–8]. If special tooling or molds are needed the time and cost for design and production of those components can be saved. Moreover, those tools often have to be stored and particularly in ceramic part production their wear is high [6,9–11]. Machining costs can make up to 70% of total manufacturing cost for ceramic parts [12]. Without the need for tooling the lead time can be reduced significantly and it makes one-time production of complex parts more affordable.

Furthermore, AM allows to produce geometries that would not be possible with conventional techniques. In some cases parts can even be printed as a whole and assembly work can be eliminated [11]. Furthermore many AM methods need less material or enable recycling of material and by doing that reduce waste which is especially appealing for working with high-value materials [7,11]. With some AM methods material or functional gradient structures e.g. from porous to dense can be realized [13,14].

To sum it up the main advantages of AM are higher freedom of design, reasonable costs for single or low volume part production, material or functional gradient, reduced lead times and possible less assembly work. Those benefits can for ceramics for instance be exploited for medical applications or components for aerospace, engines or electrical parts [5,15,16]. Especially for implants which are individual parts for each patient AM can be a great opportunity and is already used in practice [17,18]. Other common applications are turbine blades or propulsion parts due to the increasing application temperatures and dentistry. Part requirements like size, resolution and surface quality together with the material available for the special AM processes are the main criteria for the selection of an AM method for the production of a special part.

In the focus of this work are the powder-based technologies binder jetting and powder bed fusion and the built up of a dense powder bed for those processes. These powder bed methods are especially interesting for printing of larger parts with a reasonable surface whereas other AM methods like stereolithography and inkjet printing are more suitable for small precise parts or material extrusion is an interesting method for porous parts or parts with tolerance for very rough surface structures. For binder jetting printers with a build volume of $4 \times 2 \times 1$ m exist which is way larger than for most other AM methods excluding material extrusion systems [19]. In the following part the two powder-based AM techniques with focus on the powder bed formation are described. Part inscription by laser application or binder jetting are not taken into consideration. Du has written a review about all process steps of binder jetting process whereas this review focuses on the powder bed density for powder bed fusion and binder jetting and the different factors influencing the density [104].

1.2. Powder bed fusion

C. R. Deckard developed and patented selective laser sintering (SLS) as the first powder bed fusion method at the University of Texas at Austin, USA [20]. The process consists of 1) powder layer deposition and 2) selective fusion between the powder particles by raster-scanning with a high power energy beam laser and 3) repetition of steps 1) and 2) to build up the parts layer by layer [3,21,22]. Typically a laser is used as a heat source, but recently other heat sources like electron beams are reported also for ceramic powder bed fusion [21,23,24].

There are different mechanisms for the joining between the powder particles: a) full melting, b) liquid phase sintering or partial melting, c) solid state sintering, d) chemically induced binding or e) gelation reaction (i.e. the formation of a three-dimensional network that entraps the powder) [21,25,26].

A common term to indicate processes in which the material is not fully melted is selective laser sintering (SLS), whereas processes in which the material is fully melted are sometimes also named selective laser melting (SLM) [7]. All of the mentioned mechanisms have been used in the literature to make ceramic parts, even full melting which is difficult due the occurring high thermal stresses that have to be controlled [26–29]. As the whole laser melted line is under tension stress management is especially challenging for ceramics which have a low tensile strength compared to metals [30]. Moreover, metals have a one to two orders of magnitude higher value for fracture toughness and generally lower melting points therefore managing thermal gradients and thermal stresses for ceramics requires higher temperatures of build platform and build chamber [26–28]. Thermal stresses can also be reduced by decreasing sample height, adapting exposure strategy and using pulsed lasers [26,27,31].

Liquid phase sintering of ceramics is either performed with a) a mixture of ceramic particles with a binder [32], b) with ceramic particles which are coated with a polymer [33], c) by using materials such as silica or metabolic acid which form a liquid glass phase [34,35] or d) by ceramic materials showing a relatively low melting point like MgO--$CaMgSiO_4$ [36].

Laser sintering by a gelation reaction is a rarely used process but was for example proven by Liu et al. for SiO_2 [37].

Chemically induced sintering is based on a thermally activated reaction either between two powders or between powder and atmospheric gas. It was for example used for laser processing of SiC in the presence of oxygen. During the reaction SiO_2 is formed and a composite of SiC and SiO_2 emerges [38]. A similar process was applied for the production of AlN by selective laser sintering aluminum powder in the presence of nitrogen [39]. For liquid phase sintering there is often a combination of structural and binder material used which can be applied as two separate powders, as composite particles or as coated particles [21,25].

When preheating is necessary to reduce the temperature differences between powder bed, process chamber and process zone, overall part construction time can be relatively long [7]. Due to the high temperatures needed high power is required for PBF [40]. Properties of parts produced by PBF can for instance be improved by infiltration [41], annealing [42] or cold isostatic pressing [43–45].

In SLM/SLS the powder bed properties can have a strong influence on the printing parameters and the final part properties. The laser absorption on the powder is dependent on the material, powder shape, size and distribution as well as on powder bed density and powder bed thermal conductivity [7,46]. Powders offering a high surface area usually allow high absorbance of the laser energy. Highly packed powder beds show improved thermal conductivity compared to low density beds and in the end improved mechanical properties [7,47]. Mechanical

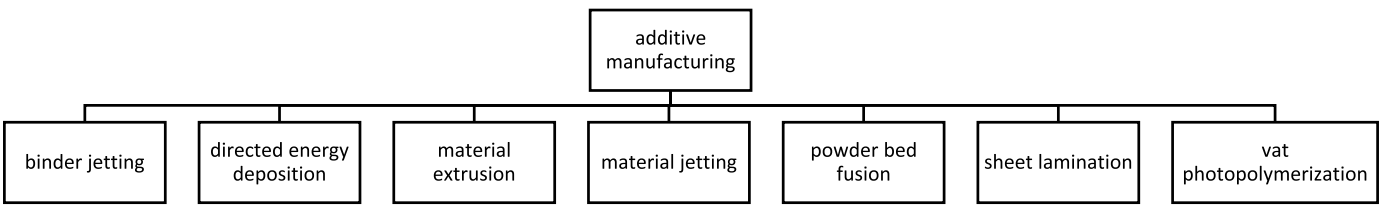

Fig. 1. Seven groups of AM defined by ASTM 52900 [2].

properties are, especially for ceramics, strongly influenced by defects like cracks caused by thermal stresses during the process. To allow heat to be transferred away from the part and avoid such stresses for many materials support structures are required that prevent local overheating and excessive warping [7,48]. Such support structures are not necessary in binder jetting as no heat is applied. On the other hand the production of already finished parts that do not need further heat treatment are possible by powder bed fusion [29].

1.3. Binder jetting

Binder jetting was patented in 1989 under the name of Three-Dimensional Printing (3DP) by Sachs [49]. In binder jetting the part is built by the following steps: 1) a thin layer of powder is spread, 2) liquid binder is jetted from the print head onto the powder layer where an object is to be formed in accordance with the layered CAD model. In many cases the binder is partially cured or dried before the next layer of powder is spread and the part is subsequently built up layer by layer in this fashion [7].

Almost any material can be used for binder jetting in contrast to powder bed fusion technologies where heating, which could lead to residual stresses, phase changes or oxidation, is applied [50,51]. The technology is easily scalable and allows high production rates (compared to powder bed fusion) and large build volumes [19,51–53]. Furthermore, in contrast to powder bed fusion or material extrusion, support structures are not necessary, thus eliminating the need for additional removal steps [51]. In addition to that no high power energy source is necessary and porosity can be controlled in certain ranges [51]. Machine costs compared to powder bed fusion machines are also cheap. A drawback of binder jetting is the need for post-processing steps which poses the risk of distortions due to asymmetrical densification or undefined shrinkage, which can prevent reaching the desired dimensions. Nevertheless, for ceramics the post-processing process has to be developed for every material anyway. Moreover, other AM technologies show higher accuracy and better surface finishing of the produced parts [51].

2. Powder bed density

For the production of dense ceramic parts using binder jetting or powder bed fusion the most important factor is the powder bed density. Only a high and homogeneous density of the green parts allows the parts to sinter to full density. Furthermore, during the build of the part a high packing promotes a stable support for the part being in built and prevents sinking of the parts in the process [54]. Some works focus on increasing the final density of the parts during postprocessing by modification of the powder so that it densifies more easily during sintering. This can be achieved for instance by the formation of liquid phases [55], infiltration of the porous part [56–59] or cold or warm isostatic pressing before sintering [60,61] similar like post processing methods mentioned for powder bed fusion. However, all these methods are extra steps that require changes to the material, carry the risk of changes in geometry, cost money and time, or limit the part geometry. Therefore, a high powder bed density should ideally be obtained already in the printing process. Sinterability and the support given by a dense powder bed during printing emphasize the importance of a well packed powder bed. Powder spreading devices have been developed over the years with the aim of increasing the powder bed density and of enabling the use of finer powders, resulting in several different methods that can be used today [6,7,51]. Besides standard dry powder deposition technologies, the use of particle suspensions (slurries) as feedstock has also been proposed as an alternative particularly for fine powders. This possibility was already described in the first patent on the binder jetting process (called 3DP) by Sachs [53].

In this work, an overview on layer application technologies, considering powder spreading as well as slurry deposition is given, with the focus on powder bed density.

2.1. Powder-based layer deposition

The powder bed density of beds made by layerwise spreading of powders is influenced by many parameters which can be seen from Fig. 2.

The parameters can be grouped into three main categories consisting of flowability, powder properties and deposition process [62–66]. Of course, many parameters influence one or more of those categories and in some cases, they interfere with each other and cannot be considered as independent. The effect of those parameters on powder bed density and their interactions are explained in the following part. Additionally, the effect on other aspects which are important for binder jetting or powder bed fusion process and the final part properties are only briefly mentioned.

2.1.1. Powder properties

Fig. 2 shows that there are many parameters influencing powder bed density, such as chemical composition, material density, electrical properties, and particle shape [67] but also compressibility, roughness, particle size as well as particle size distributions. The chemical composition determines surface charges and thereby the adhesion and respectively the repulsion between particles [66]. Furthermore, the chemical composition determines the material density. The density is important as it is directly related to the gravitational force [66]. The electrical properties of a powder are of interest as the electric potential of the particle surface defines the electrostatic forces. Electrostatic charges are distributed differently for conductors and insulators. As the electrostatic forces do not decrease as much with increasing distance compared to van der Waals forces and liquid bridges, they are the dominating force at larger distances (range of about 100 μm) [66].

Another parameter effecting the powder bed density is the com pressibility. Compressibility describes the compaction related to the applied consolidation stress. In the powder bed process this consolidation stress is caused by the roller or blade spreading the powder, even though the stresses involved are much lower compared to classical powder pressing (uniaxial or isostatic), in which pressures of tens to hundreds of MPa are common. If a powder compacts under lower consolidation stresses the compaction is more effective [66].

Moreover, a surface treatment of the powder particles, a coating or a mix with a flowing agent have an effect on the behavior of the powder [68,69]. Eventually also the moisture content of the particles can have a tremendous influence on interparticle forces and therefore on flowability and behavior of the powder in the deposition process [66,70].

Most discussed in literature is probably the impact of particle size and particle size distribution on powder bed density. The upper limit of the particle size is given by the layer thickness. It is recommended that the maximum particle size is half the size of the maximum layer thickness [71]. If the ratio of layer thickness to particle size increases further the quality of the layer in terms of packing fraction and surface quality improves as boundary effects decrease [71]. Generally, the use of fine powder is said to enable parts with low porosity. However, there is not only an upper limit but also a lower limit, even though not as easy to determine than its counterpart. With decreasing particle diameter interparticle forces and friction increases and can promote agglomeration and thereby impede the flow behavior. Below a certain particle size van der Waals forces become more dominant over gravity. This is described in several scientific articles and summarized in the reviews from Nagarajan et al. [72] and Sutton et al. [73]. The highest random close packing for hard mono-sized spheres is 64% [74]. This theoretical value is often not reached in practice owing to flowability aspects related to interparticle forces. Gregorski experimentally tested by deposition with a vibrating counter-rotating roller that this max imum value for the packing density can only be reached for particles larger than 20 μm. Due to the experience gained by his experiments Gregorski suggests not to use particles smaller than 10 μm as lower limit [75].

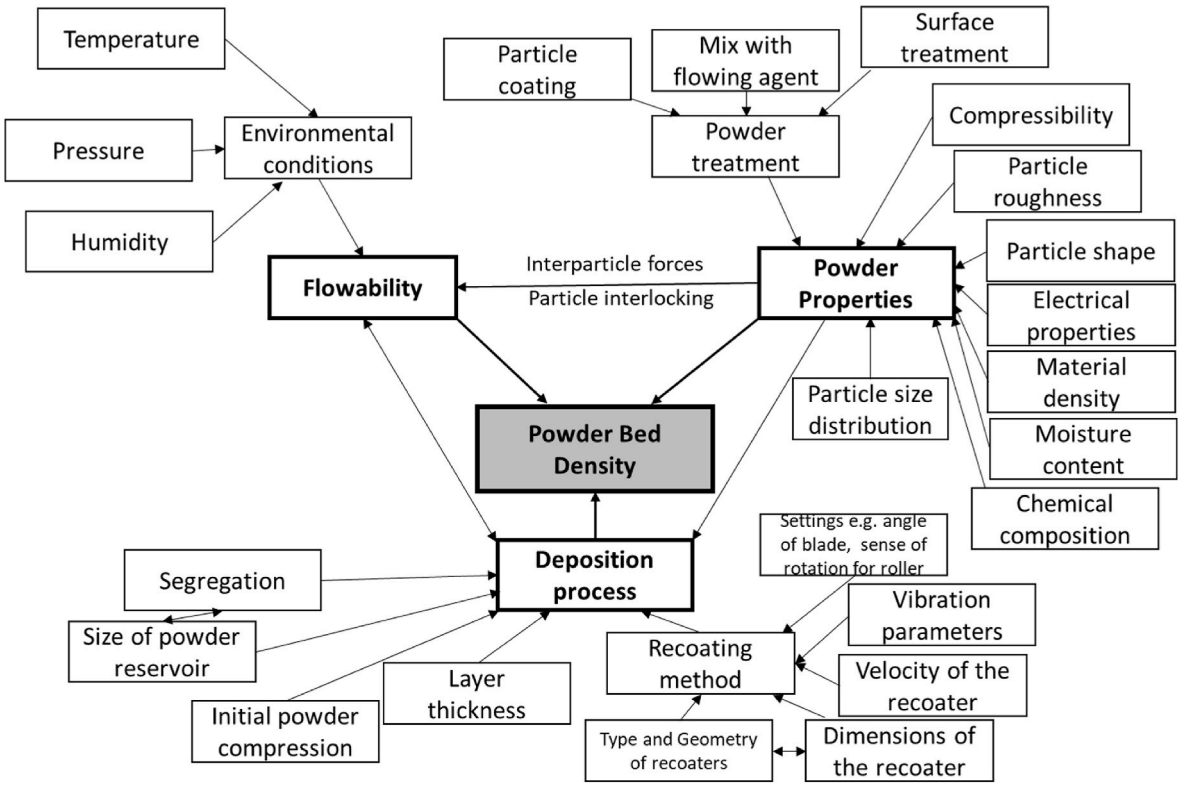

Fig. 2. Parameters influencing powder bed density.

A mixture of fine and coarse particles can increase the packing as the fine particles can fill the voids between the coarse ones [7]. The optimized composition of such bimodal distributions for different diameter ratios was calculated by several researchers [75–78]. In their easiest form those investigations assume spherical particles for the calculation of an optimized particle size distribution for high packing density. Even higher packing densities can theoretically be reached using trimodal or continuous modal distribution [75]. Meaning a broad particle size distribution can lead to a dense powder bed if segregation can be avoided. However, those models do not consider interparticle forces gaining importance for small particle sizes and are therefore more relevant for coarse particles. Furthermore particle shape is not taken into account for the mentioned calculations. There are some calculations available for powders with shapes different from spherical geometry. Man et al. for instance calculated that ellipsoids with an axes ratio of 1.25 to 0.8 can reach a packing density of about 74%, showing that non spherical but regular shaped particles can pack as dense or even denser than spheres [79]. In practice however it is usually observed that non-spherical particles pack less dense than spherical particles [80]. Nevertheless hitherto no general correlation was reported between particle shape and packing density as there are too many influencing factors which have to be taken into consideration [80]. However, a higher deviation from a spherical shape is accompanied by higher friction and interlocking effects that hinder the densification. Naturally, interlocking forces are more important for irregular shaped particles whereas particles with a round and smooth surface roll and slide more easily against each other [81].

Zheng et al. introduced a model to calculate packing density respecting particle size distribution and particle shape with certain restrictions and predictions [82]. Even for such models which are taking into account many parameters, it is critical to put the theoretical results into practice. One reason for that is the determination of particle size distribution and shape of a powder. Especially size distribution depends on measurement system and particle shape. Additionally, for practical applications in additive manufacturing, it is indispensable to check the availability of particles with the desired morphology as not all materials are provided in the ideal shape for powder spreading.

Apart from the perfect powder for particle packing in additive manufacturing equipment the particle size distribution is also important for the sinterability of the powder and layer smoothness. Sinterability is improved with increasing surface area coming along with smaller particle sizes [83]. Granulation of fine powders (below 10 μm) can be an option, even though when using granules the packing density in the powder bed is not homogeneous, which can cause problems during printing or later in the sintering stage [83–86].

2.1.2. *Flowability*

As already mentioned above very fine or irregular shaped powders are hindered to flow and thereby to arrange in a compact powder bed by interparticle friction and forces. Different other parameters like environmental conditions and characteristics of the powders (such as surface energy) or the deposition process (such as applied force) influence the flowability by counteracting the adhesive forces between the particles [66,81,87]. Therefore, one can conclude that flowability is not an inherent powder property but more an “umbrella term describing the complex behavior of powder, when it is mobilized or subjected to stress” [81]. Flowability is influenced by the adhesive forces of van der Waals forces, electrostatic forces and liquid bridges. van der Waals forces are due to the electric dipoles of the atoms and are strongly reliant on particle distance. Electrical potentials of the particle surfaces cause different electrostatic forces. The adhesive force of liquid bridges originates from surfaces tension that attracts the particles to each other. Flowability is crucial for uniform powder spreading [88] and thus homogenous green and sintered part structure [89]. It can be assessed by different methods like funnel, angle of repose, avalanching/revolution powder analyzer, powder rheometer, Hall flow meter or rotational cell [66,90–95]. A typical number to quantify flowability is the Hausner ratio which is the ratio of tapped bulk density to freely settled bulk density [96,97]. Another parameter often used to determine flowability is the Carr

flowability tested by measuring different angles and sieving results [66]. However, as flowability is no powder property there is no single, reliable and widely applicable flowability test due to different material parameters and varying forces used during powder handling [98]. Powder which should be used for homogeneous layer deposition usually have to be tested in real deposition tests to evaluate their suitability for the process as there is no test that could fully characterize the powder flow properties as those are dependent on the stress state [99]. Several overviews of possible measurement techniques for powder flowability are summarized in literature [66,99–101]. Therefore, a flowability evaluation is always related to the equipment used for determination.

According to the literature review of Vock et al. there are three trends for the relationship between powder properties and flowability [81].

- The narrower the particle size distribution the better the flowability [81].
- Flowability improves with increasing particle size [81]. As Fig. 3 shows with increasing particle size x the influence of the weight of the particle and therefore gravitational force increases which supports good flowability [66]. However, a general statement on the influence of particle size is not possible as e.g. width of the particle size distribution and particle shape have to be considered [66].
- Increasing moisture content impairs the flowability until saturation with liquid [81]. Moisture causes liquid bridges which increase interparticle adhesive forces because of their surface tension and a possible negative capillary pressure [66]. The growing adhesive forces reduce the flowability. On the other hand moisture can act as lubricant and enhance the flowability if the saturation level of the powder is exceeded [102]. In addition to that the moisture can increase the electrical conductivity of the powder and thus decrease electrostatic charging [103]. The possible effects of moisture on the flowability are illustrated in Fig. 4 [66].

Considering the demands concerning particle size to obtain a high packing density in the powder bed one can see the contradictory requirements. A wide particle size distribution theoretically allows a dense stacking of the particles but will be opposed by a low flowability, and on the other hand highly flowable coarse particles do not allow a high powder bulk density. A trade-off has to be found for particle size and particle size distribution to reach the overall best results [77].

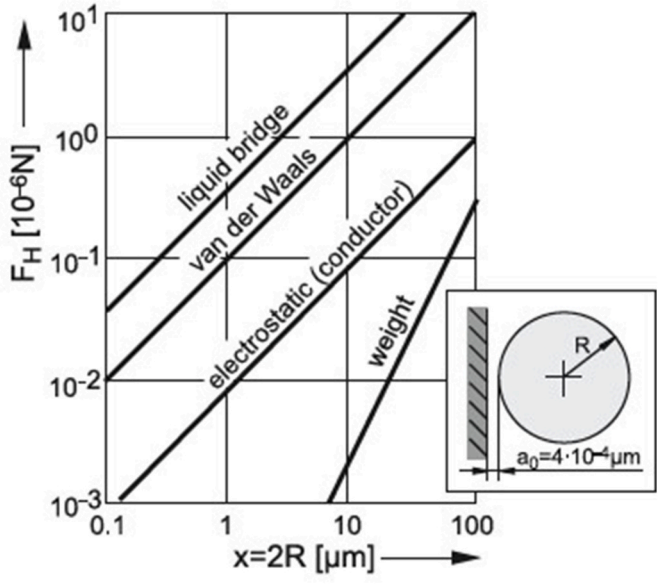

Fig. 3. Interparticle forces F_H dependence on the particle size x [66].

No general relationship could be found for other parameters affecting flowability such as particle shape [66]. Increasing particle roughness seems to decrease flowability (see Fig. 5) [32,41]. Electrostatic forces and van der Waals forces are affected by temperature and humidity as well, also impacting flowability [70]. Additionally, pressure and pressure changes for example in the powder reservoir can change the flowability of a powder. In his review Du demonstrated that all kinds of particle shapes were used for printing [104].

The flowability of a powder can be improved by powder coatings [68] and surface treatments like chemical vapor deposition or plasma treatment [88,106] or it can be improved by additives in the powder mixture [107,108]. Some researchers used flow agents to improve the flowability of the powder. Those work by decreasing the friction between the particles by serving as a low friction media [109] or by decreasing the adhesive forces between the particles increasing the distance between the particle [66]. In both cases the flow agents prevent the particle surfaces from direct contact [66]. For a porcelain powder Miyanaji and Yang for example mixed up to 10 vol% Aerosil R 972 hydrophobic fumed silica powder with an average particle size of 16 nm to the used porcelain powder to reduce the aggregation [110].

Ideally in the powder bed processes a powder flows well during powder deposition, but remains in place after positioning to avoid flaws or irregularities in the powder bed and offer a stable foundation for the printing process [86,88]. A method to achieve this powder behavior was presented by Gregorski by utilizing a metal powder that was coated with a salt. This led to a high flowability in dry conditions but low flowability in a humid environment [75]. The coated powder was spread as usual and then moisture was applied onto the layer to basically interlock the particles [75].

Flowability is also important for depowdering as powders with high flowability facilitate the removal of particles from undercuts and cavities [88]. If powders are locked or highly densified depowdering is more difficult. Eventually, the surface quality of the printed part is also related to a particle size distribution and flowability because a highly flowable powder results in homogeneous and smooth layering [71].

2.1.3. *Powder spreading systems*

There are several powder spreading devices to deposit powder beds. According to Gibson et al. [7]. they have to fulfill four aspects:

1) the reservoir has to provide sufficient volume for the whole powder bed or a smaller reservoir has to be feeded by a larger one periodically to guarantee enough material for the layer deposition;
2) the correct volume has to be applied for each layer to enable a full layer but limit excess material;
3) the spread powder layer has to be smooth, thin and repeatable;
4) the spreading mechanisms must not cause high shear forces that disturb previously deposited layers.

The basic designs of powder spreading systems are hoppers, blades and rollers. For all those raking systems the forces applied on particles are limited and therefore optimized flowability and powder properties to build a dense powder bed are important. The most commonly applied basic devices (hopper, blade and roller) are shown in Fig. 6 and explained in further detail with special focus on their effect on powder compaction and thereby powder bed density. The achieved powder bed density for each of those powder spreading devices is dependent on the used powder, flowability and parameters for deposition. A parameter to be selected for all spreading systems is the layer thickness. Other parameters to be selected depend on the raking system. For a roller spreader for instance velocity of the recoater, sense of rotation of the roller or diameter of the roller influence the packing of the powder. For a hopper parameters like size of powder reservoir and possible vibration have to be optimized. This range of impact factors makes a comparison between the different systems complicated. Here information available

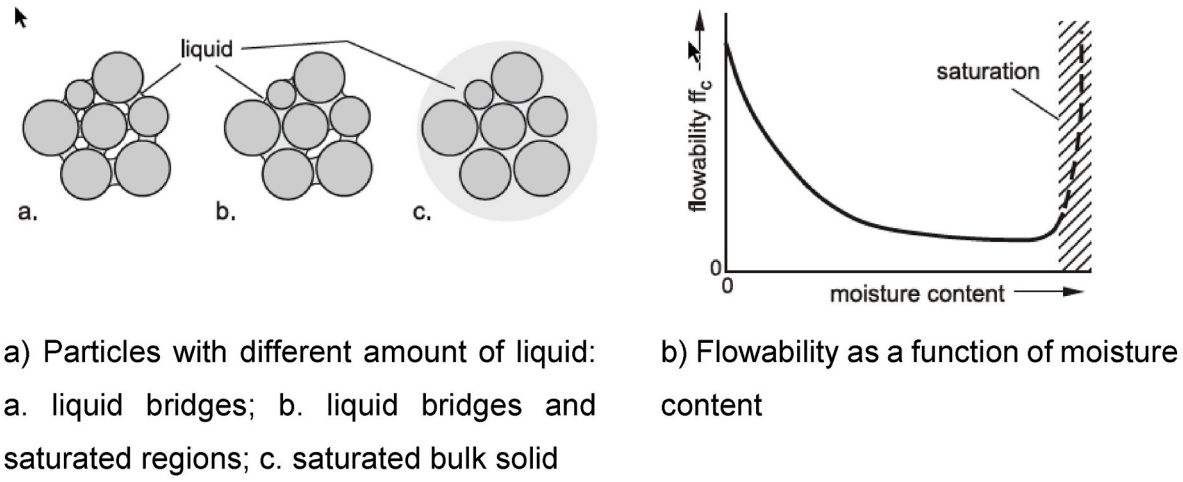

a) Particles with different amount of liquid: a. liquid bridges; b. liquid bridges and saturated regions; c. saturated bulk solid

b) Flowability as a function of moisture content

Fig. 4. Flowability effected by moisture due to liquid bridges [66].
a) Particles with different amount of liquid: a. liquid bridges; b. liquid bridges and saturated regions; c. saturated bulk solid b) Flowability as a function of moisture content.

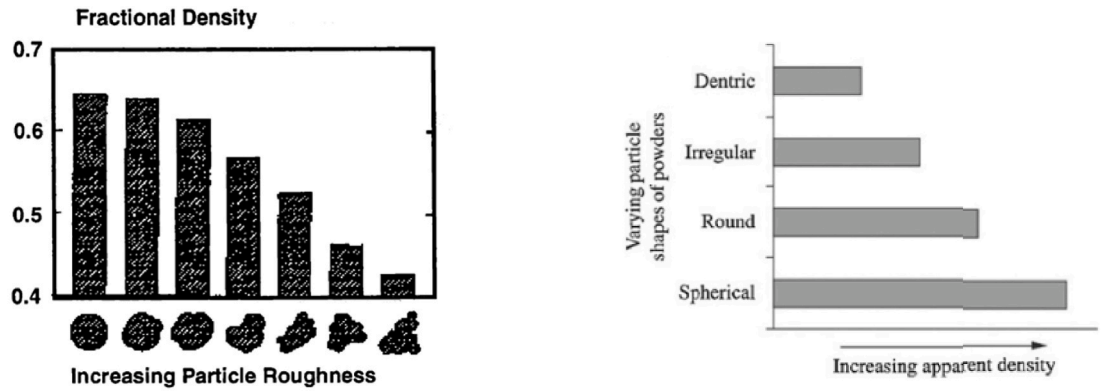

a) Fractional packing density versus relative roundness for randomly packed mono-sized particles [76].

b) Effect of powder morphology on apparent density (this assertion is only true with a fixed particle size) [105].

Fig. 5. Packing density or apparent density in dependence of particle shape.
a) Fractional packing density versus relative roundness for randomly packed mono-sized particles [76]. b) Effect of powder morphology on apparent density (this assertion is only true with a fixed particle size) [105].

in the literature about the different devices are collected to provide some guidelines for the selection of the deposition method and parameters. For each powder material the optimized parameters need to be experimentally tested due to the lack of an easy calculation method, as there are too many parameters influencing powder bed density. Several researchers have conducted such studies based on simulations and experiments [111,112]. A comparison of some of the mentioned deposition devices is also provided by Nagarajan [72].

2.1.3.1. Basic powder spreading devices

Hopper

A hopper (s. Fig. 6a) is a dispenser that distributes the powder while travelling across the bed. Such a system was used in several binder jetting machines and variations of it such as a combination of hopper with a blade (s. Fig. 6b) were patented [113–116]. The hopper feeding system uses a reservoir above the powder bed. To fluidize the powder, the hopper shakes and deposits the powder in front of the spreading tool [115]. The powder conveying in the hopper can be improved using vibration [117]. Kumar et al. have simulated that a higher vibration acceleration amplitude and frequency causes a faster particle velocity during hopper discharge. However, it has to be avoided that fines content does not stay in the hopper due to segregation induced by vibration [47]. The influence of the filling systems of the hopper is described by Guo and Leu [118]. Different vibration dry powder-dispensing systems are summarized in Nagarajan's review [72]. Multi-material parts can be made by using multiple hoppers with different materials and changing the material layer by layer [119]. The company Aerosint shows another method for printing multi-material parts: a recoater which uses patterning drums which selectively deposit fine powder voxels in a line-at-once-manner. The final layer can be composed of more than one powder material [120].

Blade

A simple thin blade or knife can also be used to drag and wipe off the powder at a certain distance to the building plate or previous layer. It needs to be at least as long as the width of the powder bed. Scraping causes high shear forces in the previously deposited layers [7]. Those forces can be reduced by applying ultrasonic vibration to the blade [72]. Examples of this type of powder spreader are found in U.S. Pat. No. 5, 387,380 to Cima et al. [121] and U.S. Pat. No. 6,799,959 B1 to Tochimoto and Kubo [122]. Furthermore, if the blade is uneven this will be transferred to the powder layer evenness. There is no densification of the powder with the typical blade geometry [123]. Haeri therefore designed alternative geometries of blades. The best result was achieved with a

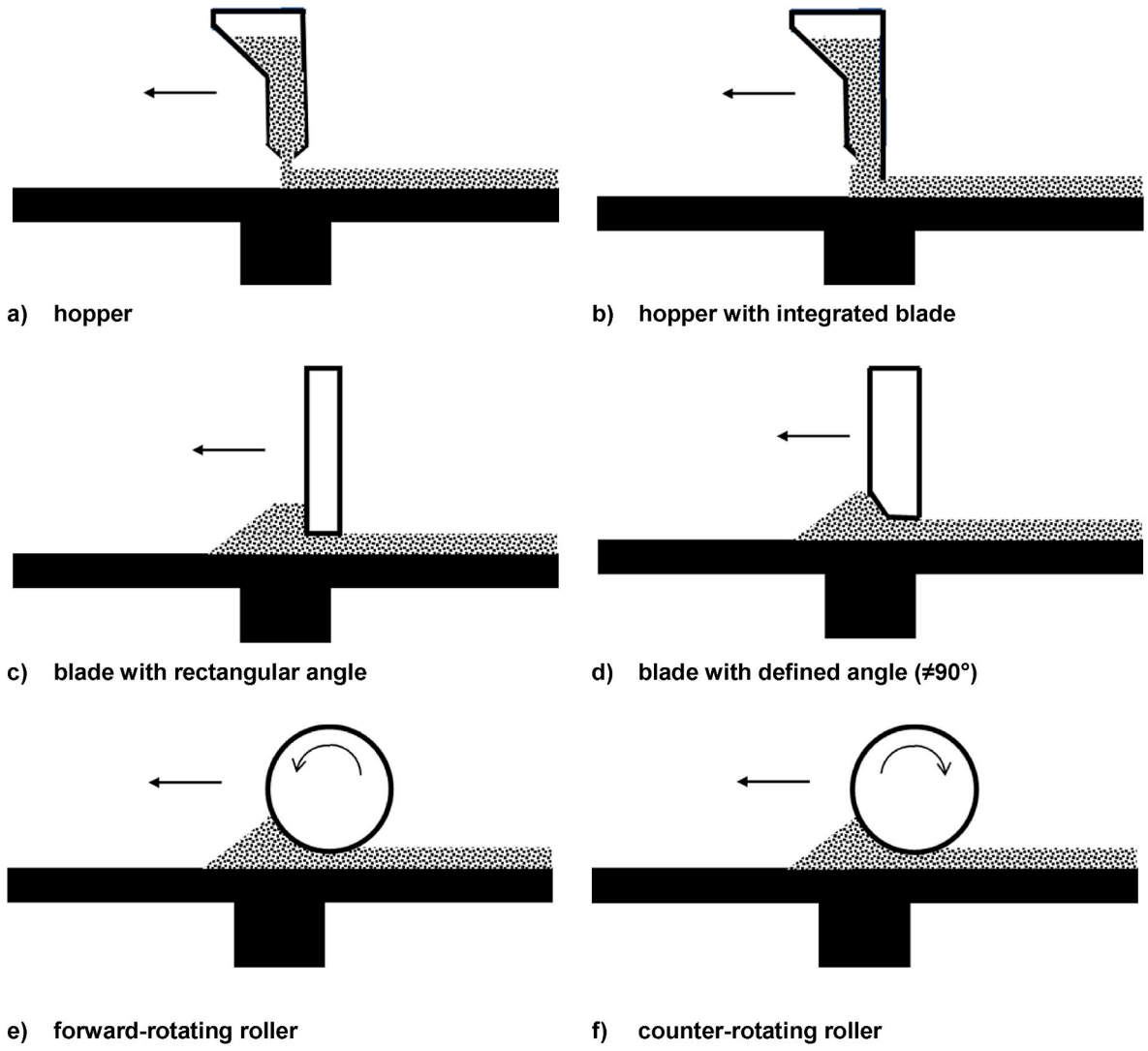

Fig. 6. Basic powder spreading devices: a) hopper, b) hopper with integrated blade, d) blade with rectangular angle, d) blade with defined angle (≠90°), e) forward-rotating roller, f) counter-rotating roller.
a) hopper b) hopper with integrated blade.
c) blade with rectangular angle d) blade with defined angle (≠90°).
e) forward-rotating roller f) counter-rotating roller.

blade with a super-elliptic edge profile that applies higher forces on the powder which allows a comparable compaction than the roller based devices [124]. Gregorski presented a new deposition apparatus in his thesis with a wedge that has an angle of 45° [75]. The operating principle is the same as the one shown in Fig. 6d.

Different blade geometries with flat, round and sharp edges were tested by Beitz et al. to optimize the surface quality of the spread layer. A flat bottom shape provides the smoothest surfaces. No information was submitted on bed density [125]. For blades the geometry, layer height and speed of the blade can be changed to alter the effect of the spreading on powder bed quality [88]. The velocity of the blade has a great impact on the powder bed density. The optimized blade geometry from Haeri enables a faster printing process while keeping highly dense layers [124]. According to Haeri the improved super-elliptic blade geometry produces smoother surfaces [124].

Forward rotating roller

A forward rotating roller (s. Fig. 6e) is a roller that rotates in the same direction as the traversing direction, i.e. the movement is the same that the roller would make if it were simply being rolled across the powder bed surface. The powder is compacted by the traversing movement, while the rotation smooths the powder bed [126]. A high compaction is achieved as relatively large forces act on the layered powder [127]. Due to this densification process agglomerates can occur that stick to the roller and leave voids in the spread layer [87]. Hence, the use of forward rotating rollers carries the risk of incorporating holes in the layer and therefore the forward spreading roller is barely used. Parameters that influence the powder spreading are layer thickness, diameter of the roller, roller contact pressure, roller angle, friction between both roller-powder and powder-powder, speed of both, the forward movement and rotation of the roller [111]. It is known that with increasing diameter of the roller the compaction improves [87]. According to Budding and Vaneker neither linear nor rotational velocity of the roller have an influence on layer density [87]. Whereas Drummer [128] states density improves with increasing velocity and Haeri's [123,129] simulation and experiment claim the opposite. If the rotational velocity of the roller is low, however, the roller will have the same effect as a blade [87].

Counter rotating roller

The counter rotating roller (s. Fig. 6f) rotates in the direction opposite to the forward movement of the roller. Akin to the forward

rotating roller, it deposits the powder during movement of the roller above the powder bed. However, it does not show the creation of voids due to sticking powder on the roller. Moreover, in this case the sticking of the powder to the roller functions as a pick up and redistribution of the powder [115]. The roller movement thereby stimulates the powder flow in front of the roller and enables a powder distribution with almost no destruction of the previously deposited layers is noticed [72]. Surface roughness is expected to be low [124]. For these reasons this is one of the most widely used powder spreaders in industrial AM [130]. Nevertheless, the densification provided by counter rotating rollers only works up to a certain roller size as the fixation points can only be at the ends of the roller. Usually, the maximum diameter should not exceed about 5 cm as otherwise the compaction might increase to the point that previous layers would be destroyed. This small diameter combined with a long roller leads to bending and flexing of the roller during the deposition and therefore an inhomogeneous and uneven powder bed. Even a roller of about 30 cm length and 5 cm diameter exhibits intolerable deviations in the deposited layer [115]. Parameters that can be altered are identical to the forward rotating roller. A similar method to the counter rotating roller but with less requirements regarding electrical or magnetic properties of the powder using a strip of flexible material for deposition is presented in US 8,568,124 [115].

2.1.3.2. Variations, modifications and combinations of the basic spreading systems

There are several ideas on combining and modifying the mentioned basic spreading mechanisms with each other to increase powder density or obtain smaller layer thicknesses.

Vibrated spreading

In many cases compaction of the powder bed is supported by vibration [75,131,132]. Density can be increased enormously by the application of small amplitude and frequency [131]. Vibration can be applied by the build platform, the powder bed surface and the blade or roller [132]. Very often the roller is vibrated. Amplitude and frequency of the applied vibration have to be optimized to achieve a dense powder bed [69]. Nonetheless, vibration can also cause defects like ridges [68]. As a solution a two-step spreading process is recommended: First a prelayer is spread by means of vibration and then a second pass without vibration smoothes the surface. Even though this method works the build rate is decreased which has to be avoided. Two closely spaced rollers with the first vibrating and about 10–30 μm higher than the second non-vibrating one are a better solution [68].

Combinations of rollers

This spreading mechanism is a combination of two counter rotating rollers (see Fig. 7a) to achieve ultra-thin layers (about 50 μm) and enable the use of fine powders. Thinner layers may be desirable to reach a better surface quality or higher accuracy. Making ultra-thin layers using a simple counter rotating roller often creates cavity defects or part-shifting defects as the particle size has to be very small and van der Waals forces gain in importance compared to thicker layers. To avoid such problems the double action roller is applied [130]. In principle the double action roller creates an interim layer which is slightly higher than the final layer and then a second counter rotating roller movement brings the layer to the desired final thickness [130]. According to Cao the green density of alumina increased from 43% to 70% by using this double action roller instead of a vibrated rotational roller [130]. However, the time for layer deposition is longer as there are twice as many roller movements than in counter or forward rotating roller powder spreading. Small layer heights as proposed by Cao additionally increase the building time but on the other hand offer higher accuracy [130]. A similar process with additional application of vibration to the roller was already introduced at MIT in the 1990s under the name of press rolling

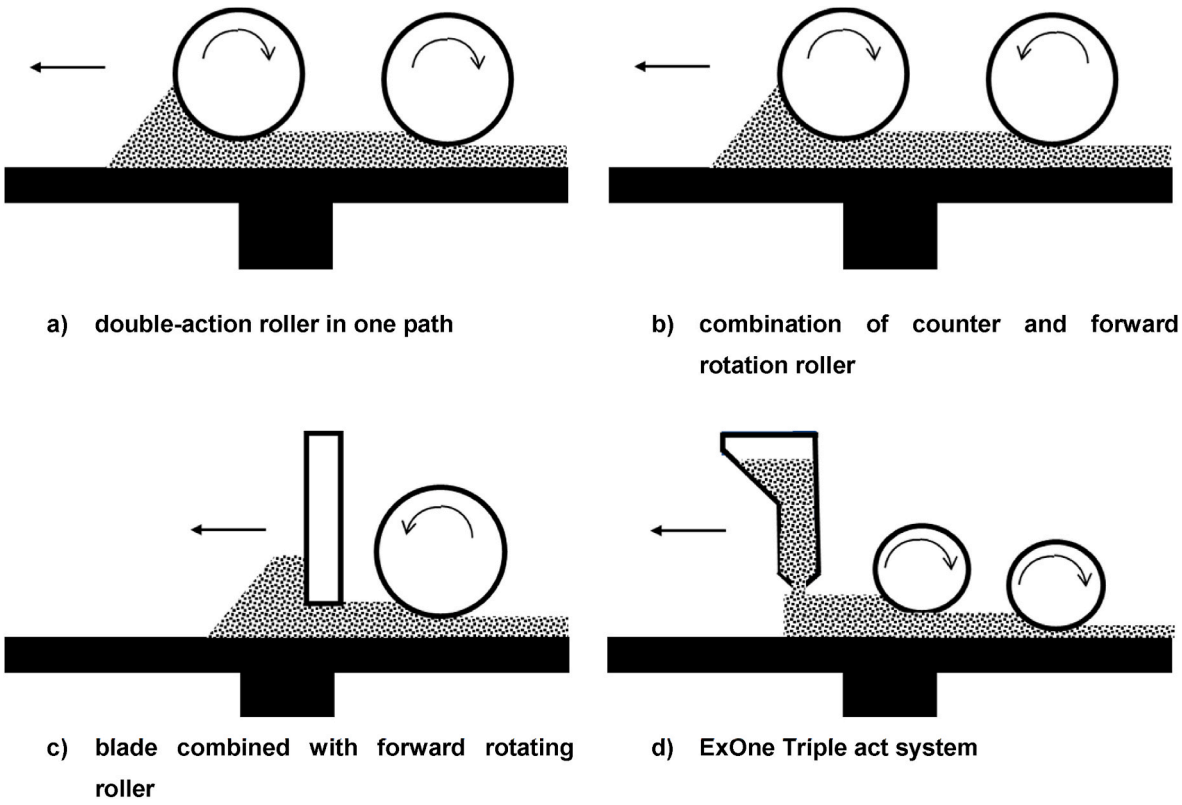

Fig. 7. Modifications and combinations of basic powder spreading devices: a) double-action roller in one path (could also work in forward and backward movement with one roller), b) blade combined with forward rotating roller, c) ExOne Triple act system.
a) double-action roller in one path b) combination of counter and forward rotation roller.
c) blade combined with forward rotating roller d) ExOne Triple act system.

technique [60]. The piston first spreads the powder with a layer thickness slightly higher than desired and on the return pass a load is applied to compact the powder. Thereby powder bed densities of about 40% were obtained [133]. Niino and Sato suggested the use of counter rotating roller followed by a forward rotating roller like it is demonstrated in Fig. 7b.

Combination of blade or hopper and rollers

The problem of limps sticking to the forward rotating roller and creating craters in the next layer can be eliminated by producing a prelayer with a slightly higher layer thickness than the final layer height using a blade and then compacting everything by the forward rotating roller. This combination of a blade and forward rotating roller is schematically shown in Fig. 7c and was suggested by Budding and Vaneker [87]. Hence, the high compaction achievable by forward rotating roller can be exploited [87,134]. However, some optimization is still needed to prevent voids completely [87]. Parameters that can be altered are the ones for rollers, blades and the extra height of the prelayer.

The company ExOne provides binder jetting machines with a so-called triple act system where an ultrasonic hopper is combined with a roller system (see Fig. 7d). The powder is deposited on the layer with the hopper and then leveled with a spreading roller and finally densified by a compacting roller [52].

Some more extra ordinary spreading devices can be found in literature. Haferkamp et al. combined three rollers in a triangular arrangement [135]. Regenfuss et al. dispersed and compacted powders by a combination of a compaction cylinder with a blade [136].

Gas flow assisted deposition

Another possibility to increase the density of the powder bed is the application of a gas flow through the powder bed and the building platform, so that the particles are drawn to the bottom. This method was introduced to prevent the displacement of parts due to shear forces affecting them during deposition of the next layers. It was also proven to significantly increase the powder bed density, especially for fine and poorly flowable powders [137]. It is described in more detail in Patent US953345B2 [138]. Chinellato et al. applied this method to handle fine α-tricalcium phosphate [139].

2.2. Slurry-based layer deposition

A higher powder bed density can be achieved using slurry deposition instead of dry powder deposition. Especially for particles sized smaller than one micron gravitational forces are outpaced by interparticle forces. For such particles depositing a dry smooth layer becomes difficult [68,71]. Generally those finer particles require a slower spread speed [110]. Slurry-based layer deposition in contrast to powder-based deposition allows the handling of such small powders while achieving high powder bed densities.

2.2.1. Possible slurry deposition methods

There are several possibilities creating powder beds by depositing slurries. Grau compared spray deposition, slurry jetting and tape casting [140]. In spray deposition a slurry is atomized and the fine mist of slurry droplets created is deposited. By rastering the spray nozzle across the substrate a layer is created. If an ink jet printing nozzle is used for slurry deposition Grau called this method slurry jetting [140].

As an alternative method, the need for rastering across the whole substrate area can be eliminated by using a modified tape casting method. This increases the build rate of the powder bed significantly. Furthermore, since the blade is leveling each layer to the same height regardless of the roughness of the previous layer mistakes like bumps or defects do not sum up [140]. It was observed that generally the number of pores decreased from spray deposition to slurry-jetted to tape casted layers [140].

This modified tape casting method is similar to the layerwise slurry deposition LSD method. The generic working principle of the layerwise slurry deposition can be summed up as a combination of tape casting and slip casting processes. A slurry is deposited by a blade in the same fashion as in tape casting. Each layer is dried to obtain a densely packed powder bed layer-by-layer.

Since a new slurry layer is deposited on top of a dry porous powder bed, the slurry forms a cast in a similar fashion to a slip casting process. In this sense, it can be said that the powder bed acts as a porous mould for the deposition of a new layer of slurry.

The slurry is drawn into the capillary channels of the previous layers, ensuring a high packing density and a good adhesion of the new layer to the former one [141]. At first this method of forming a powder bed was used together with laser sintering [142–144]. Later this deposition process was combined with printing of a binder on the layers like in powder-based binder jetting to generate parts. This AM method was patented by Günster and Gomes under the name of LSD-print [145].

Another slurry deposition technique based on slot-die coating and tape casting was described by Yen. He used a coater consisting of a coat hanger distribution chamber combined with a blade to form a powder bed [146]. Similar but working only by hydrostatic pressure and thereby eliminating the need for a pump is the system described in patent DE10 2017 126 274 B4 by Günster [147].

Different to processes using a powder as feedstock, in slurry-based layer deposition the critical steps usually are drying of the layers and the depowdering of the printed parts at the end of the process.

2.2.2. Drying

For defined printing on the deposited slurry layers the layers have to be dried before printing. Thus, drying is an extra step needed when working with slurries instead of powders. Drying can be accomplished from the top and from the bottom. Often both options are employed simultaneously. External heat sources cause evaporation of the liquid vehicle. Capillary forces from the previously deposited and dried layers draw water by capillary forces akin to slip casting from the just deposited layer into the existing powder bed [141]. As the liquid is rapidly drawn into the pores by capillary forces drying is much faster on porous than on dense substrates [148].

Due to evaporation of the solvent the layer shrinks leading to a smaller dried layer height in comparison to the deposited layer height. This shrinkage is dependent on the solid content. The machine, however moves up the preset slurry deposition thickness H at each layer independently of the shrinkage value. For this reason, in the LSD-print deposition method the dried layer thickness changes for the first few layers but then it reaches a constant height. This height can be approximated with equation [149] and illustrated in Fig. 8:

$$\mathrm{T}(n) = H(1 - a^n) \tag{1}$$

Where $T(n)$ is the thickness of the nth layer after drying, H is the preset slurry deposition thickness and a is the shrinkage ratio of slurry layer during drying process [149]. As a is a number between 0 and 1 a^n will asymptotically approach 0 like can be seen when calculating the limit for n tending to infinity:

$$\lim_{n\to\infty} \mathrm{T}(n) = H(1 - 0) = H \tag{2}$$

During drying the shrinkage can only occur in layer height and is constrained in layer width by the adhesion to the substrate or the previous deposited layer. This causes transverse tensile stresses during drying. If these stresses exceed the strength of the powder bed cracks occur. A single crack in the powder bed can cause several discarded green parts. Therefore cracks must be avoided by all means [148]. Cracking is a result of the interplay between capillary pressure causing compression of particles, substrate affinity causing transverse stresses due to shrinkage strain and particle network strength resisting the applied forces [150].

Most theories of drying are based on depositing layers on non-porous substrates. If a dense substrate is used this applies for the first layer but the following layers will be deposited on a porous substrate. Generally

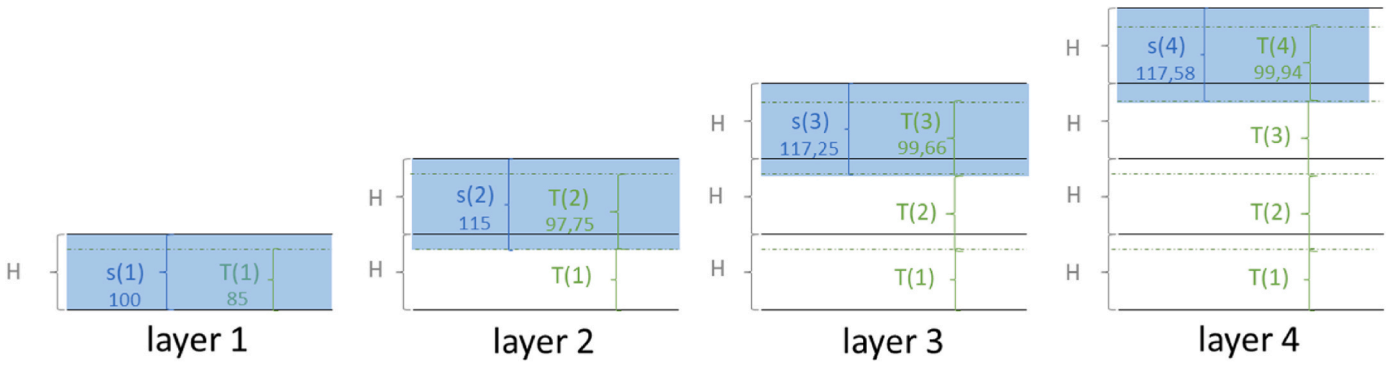

Fig. 8. Development of layer thickness according to equation.
1H: height movement of the blade according to set layer thickness; s(n): height of deposited slurry layer; T(n): thickness of nth layer after drying; numbers below the variables give a value in μm for the example of a layer height h = 100 μm and a shrinkage ratio α = 15%.

cracking occurs when the energy needed to form a crack is less than the strain energy released [151] or in other words when the drying stress is higher than the network strength (see Fig. 9)

For dense substrates a critical cracking thickness (CCT) is determined by Hu. If the layer thickness exceeds the CCT the layer will crack spontaneously during drying. The CCT is dependent on drying stress and fracture resistance of the layer (equation (3) [152,153]:

$$CCT = \left(\frac{K_c}{1.4 \cdot \sigma_b}\right)^2 \tag{3}$$

Where K_c is the fracture toughness of the layer and σ the biaxial stress.

To increase the CCT and thereby avoid cracking either the biaxial stress has to be decreased or the fracture resistance of the granular film increased or both [152].

The biaxial stress is caused by the capillary stress P_c, seen in equation (4).

$$P_c = \frac{2 \cdot \gamma_{LV} \cdot cos\theta}{r_{pore}} \tag{4}$$

Where γ_{LV} is the surface tension of the liquid, θ is the contact angle between the powder and the slurry and r_{pore} is the pore radius.

Murray claimed a better correlation of the CCT with the specific surface area than with particle size as surface roughness and internal porosity of the particle contribute to the capillary pressure [150].

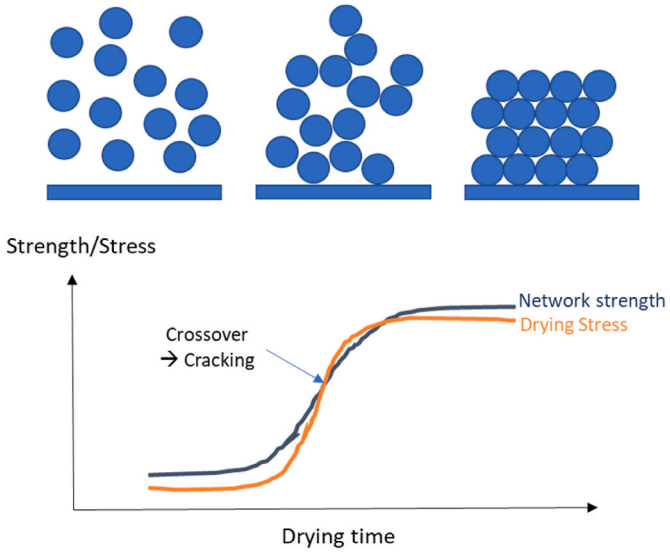

Fig. 9. (Schematically)Stress development during drying [150].

In 2007 Singh published a new method to calculate the CCT which takes into account shear modulus G of the particles, coordination number M, particle volume fraction Φ_{rcp} at random close packing, particle radius R and interfacial tension γ_{LV} between the particle and the liquid medium. In the detailed version also the sphericity of the particles is considered. However, the influence of this parameter was not significant thus the calculation of the CCT was simplified to equation (5) [154]:

$$CCT = 0.41\sqrt{\frac{GM\Phi_{rcp}R^3}{2\gamma_{LV}}} \tag{5}$$

In order to improve cracking behavior of the slurries deposited in the LSD process each of the previously mentioned parameters can be optimized such that the CCT increases. Possible alterations are explained in the following.

Fracture resistance of the layer is governed by composition and microstructure. It can be increased by organic additives as known from tape casting [148,155]. Chiu showed that the toughness of the layer can be improved by polyvinyl alcohol and that the CCT increases linearly with the content of the organic additive [152]. However, adding organic additives to the slurry in slurry-based binder jetting can be critical as the dissolution of the powder bed surrounding the green parts should be easily possible and many binders will strengthen the particle-particle interconnection [148]. Therefore, biaxial stress can be decreased by using larger particles, improving wetting or decreasing the surface tension [156].

As the particle size was chosen due to sintering requirements according to Herring's scaling law [83] the use of larger particles is usually no option. However, in some cases the addition of some larger particles can be a solution to avoid cracking. For example, a yttria stabilized zirconia slurry consisting of a nanoparticle suspension was blended with microparticles. Micro- and nanopores instead of only nanopores occurred and decreased the capillary pressure [157].

The surface tension can be decreased by changing solvent or using surfactants [152]. Grau used Triton X-100 to decrease surface tension of water from 72 to 32 dyn/cm and could thereby increase the maximum crack free layer thickness of the powder bed [140]. Another possibility to decrease surface tension is using a water/solvent mixture like water/methanol. A reduction of the surface tension of about 31% was achieved and enabled a higher layer thickness [140].

Coordination number and particle volume fraction are influenced by deposition conditions like drying conditions, which in turn are affected by humidity and temperature of the powder. These factors effect settling and therefore rearrangement time of the particles. Rearrangement of particles during settling and drying strengthens the particle network [150]. The lower the evaporation rate the denser the particle package and the stronger the network [154]. Lewis also stated that for tape casting

a slower drying rate enables better particle rearrangement and therefore a higher green density [155]. These results are in alignment with the observation of Chiu et al. that a long sedimentation time increases CCT [151]. The equations by both, Chiu et al. and Singh consider this correlation. In addtion to drying time, also flocculation changes the coordination number, and thereby final volume fraction and network strength. In a stable dispersion, capillary forces cause the particles to arrange into a dense powder bed because particles are separated in the slurry and during settling they can arrange in close packed positions and build up a dense cast. For a flocculated dispersion the forces that keep the particles apart and capillary forces are counteracting and no full densification can be reached but a porous powder bed is formed [150]. This effect is illustrated in Fig. 10. Maskara and Smith have shown that slower drying leads to higher agglomerate strength [158]. Chiu has shown that the powder bed density decrease from 62 to 54% of theoretical density when using a flocculated instead of a stable dispersion [152].

Under appropriate drying conditions there are no more residual stresses in the dried layers [151]. Prediction of the cracking behavior becomes more complex in practice as its influenced by particle segregation, stratification and percolation [150].

If a layer is deposited on a previously deposited layer as it is the case during the generation of the powder bed then the underlying substrate is porous and the drying behavior differs from that of a dense substrate. The layer is then dried by evaporation like for a layer placed on dense substrates but also by capillary effect that sucks the water or solvent into the existing porous powder bed. The maximum layer height without cracking can be described by the so-called critical saturation thickness (CST) for porous substrates.

Layers thicker than the CST crack immediately. Drying stresses are either caused by moisture gradient or by the constraints executed due to the substrate. Saturation here is defined as the percentage of porosity in the body that is filled with liquid [133].

A slurry with a low solid content will crack at low layer thicknesses whereas slurries with high solid content will not saturate previous layers so fast and allow higher layer thicknesses. Furthermore, the permeability and pore size distribution of the powder bed have an influence on CST. According to Washburn's equation the liquid transport rate is proportional to pore size meaning the higher the pore size the faster the liquid transportation rate the lower the chance of cracking as saturation is not exceeded. With increasing particle size permeability rises and thus increasing CST and facilitating the redispersion [148].

Generally, factors decreasing the capillary pressure cause an increase in CST in the same manner as for CCT. These are increasing pore size, decreasing surface tension, increasing solids content in the slurry and packing fraction of the powder bed [140]. The measured stress in the film was highest as the saturation of the film reached almost 100% [148]. Experiments on the CST were performed by rastering a jet of liquid over the surface to form the powder bed. As deposition takes some time and liquid can distribute over a longer time the effects could be different to other single-pass slurry deposition solutions [148]. High evaporation due to high ambient temperature or hot powder bed can increase the CST. The more solvent evaporates the less solvent is drawn into the powder bed and has an influence on CST.

CST considers the saturated thickness whereas in CCT the layer thickness is taken into account. Thus, they are essentially the same. Nevertheless, as the saturated region extents over more than one layer the possible layer thickness for a deposition on a porous substrate or previously deposited porous multi-layer is lower than for a single layer on a dense substrate.

Apart from cracking other problems can occur during the slurry deposition that can affect the final part quality. Layers can show bumpiness due to different cast behavior on printed and unprinted areas as the formation of the powder essentially is a slip casting process. In this casting process the solvent is sucked into the previous powder bed by

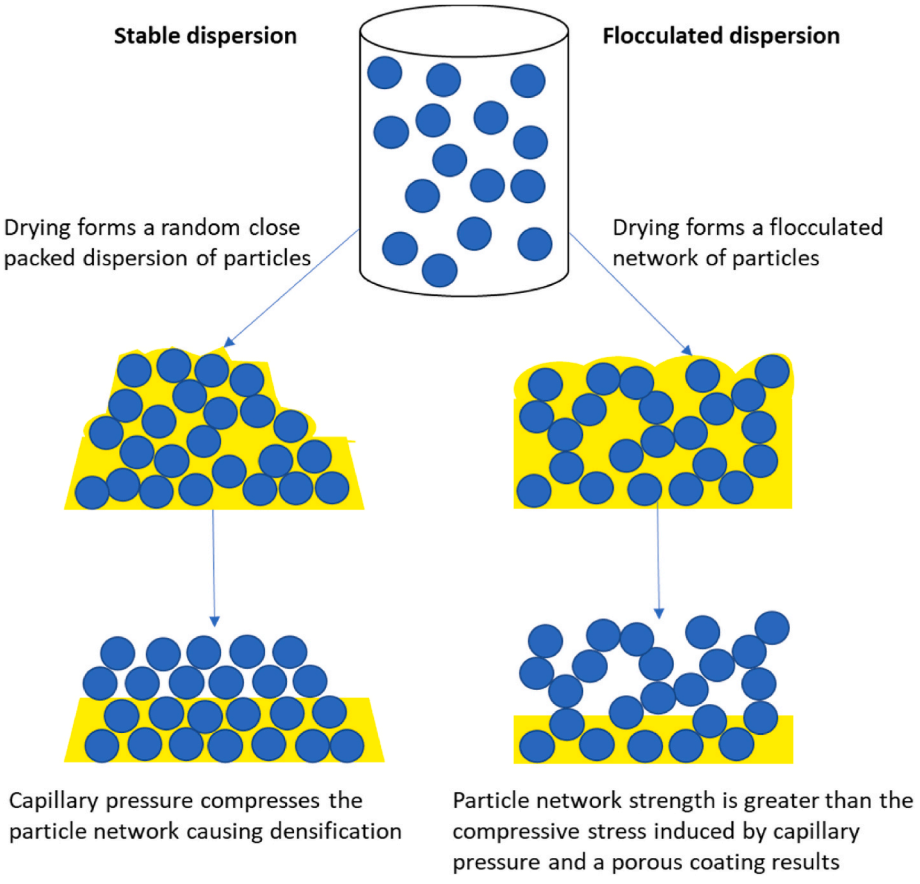

Fig. 10. Densification during drying for stable and flocculated dispersions [150].

capillary forces and the particles in the slurry build up a solid cast layer. Casting rate is influenced by capillary pressure, permeability and pore fraction of the powder bed [140]. On areas that have been printed with the binder the capillary pressure, which is the driving force for the slurry to dry, differs from the capillary pressure of areas free of binder. This causes different casting rates for those two areas and therefore changes in packing density over the layer. The lower casting rate on the printed areas reach higher packing density due to lower casting rates [140]. Furthermore, it can induce small bumps that follow from a net flux of slurry from the binder-printed region to the unprinted region [140].

Depending on the deposition method the right deposition speed of the slurry spreading device can be crucial. Khanjua for example used a tape casting method for the layer deposition. If the blade is not moved fast enough slurry in front of the blade will dry, attach to the previous layers and therefore when the blade moves on peel off portions of the previous layers [133].

2.2.3. Depowdering

The green density of powder beds formed by slurry deposition is very high which is desirable for final part properties but challenging for the removal of the unbound powder. Due to high particle-particle interactions this unbound powder sticks very strongly together. Attractive forces in binder-free powder agglomerates are van der Waals interactions, liquid bridges and electrostatic forces [66]. The use of organic additives in the slurry often also further binds the particles in the layer.

Since standard depowdering strategies for powder-based binder jetting (air suction, brushing etc.) are ineffective in this case, the part removal can only be accomplished by redispersing the powder bed [141]. For this redispersion the powder bed has to be placed in a liquid dispersion medium first. Then this medium has to penetrate into the powder bed and finally disperse the agglomerated structure into its primary particles [159]. The strength of the printed parts has to be high enough to withstand redispersion, or the binder needs to act as a diffusion barrier so that the dissolution medium is not penetrating the green body [141,159].

During redispersion several forces occur that cause the removal of powder from the powder bed. At the beginning capillary forces arise when the dry powder bed is put in the liquid. The penetrating water traps air inside the powder bed and creates a pressure on the surrounding powder bed [160,161]. Using a higher surface tension solvent this excess pressure increases. However, it should not be too high to prevent damage on parts by explosions or fast swelling. Generally the dissolution is a slow process starting from the surface and moving forward into the inside of the powder bed by removal of outer particles [141]. Therefore, it is unlikely that explosion occur [159]. However, smaller sized particles form stronger powder beds [158]. The excess pressure can be avoided or reduced by partially submerging the powder bed so that the air can leave the powder bed [140,141,159,162].

Redispersion should be carried out with a medium with a pH far from the isoelectric point of the powders as electrostatic repulsion of the particle can promote separation of the powder bed. Moon proved this when showing that redispersing a silicon nitride powder with an isoelectric point of pH 4.5 in water at pH 10 is more effective than in water at pH 6.5 [160].

The average tensile strength for powder beds without organics composed of mono-sized particles with randomly distributed cohesive forces was calculated by Rumpf [163]. Equation (6) shows that the tensile strength σ of the powder bed is related to packing fraction, particle radius, average number of contacts and the interparticle forces.

For smaller particles there are more interparticle forces and therefore the tensile strength is higher in accordance with equation (6).

$$\sigma_t = \frac{9\Phi_{rcp}}{32\pi R^2} M F_H \tag{6}$$

Where Φ_{rcp} is the particle volume fraction of the particles, R is the particle radius, M is coordination number and F_H is the interparticle force [160].

For a close-packed structure Moon [160] calculated the average number of contacts per particle (equation (7)):

$$\mathrm{M} \approx \frac{3}{1-\Phi_{rcp}} \tag{7}$$

Inserting equation (7) into equation 6 delivers the expression for tensile strength as shown in equation (8):

$$\sigma_t = \frac{27\Phi_{rcp}}{32\left(1-\Phi_{rcp}\right)\pi R^2} F_H \tag{8}$$

Grau examined the redispersion process further by redispersing slip casted samples. The weight loss of samples lying in a wire-mesh basket where loose powder can fall through was measured over time. Parameters like particle size, organic content and aging of the slurry were changed and their influence on the redispersion behavior investigated [160]. In some cases, partial dissolution and/or hydration of powders can occur. If this leads to formation of insoluble salt bridges at the necks of the particles this can obstruct the powder redispersion [160]. A stable slurry with the pH adjusted to a suitable range prevents the formation of strong chemical bonds between the dried powder particles and therefore improves redispersion [160]. In contrast to a usual dispersion process the powder bed must be redispersed without mechanical forces like ball milling [59]. The use of an ultrasonic bath could be utilized to support the redispersion [160], but care should be taken as this can damage the printed parts. Mühler suggested spray rinsing to support local dissolution of material [141]. Redispersion is effected by the medium used for redispersion, powder and polymeric additives used for powder bed formation and the slurry stability [160].

Moon tested the influence of polyethylene glycol (PEG) on the redispersion behavior with the setup described above and found out that an amount of more than 2 wt% PEG 400 in the slurry has a positive effect on the redispersion. Wherever higher molecular weight PEG was used redispersion was impeded [160]. The PEG 400 is drawn into the pores and finally settles in the point of contacts between the particles in the dried powder bed forming a soluble bridge between the particles and preventing strong direct particle-particle contacts. During redispersion the PEG 400 dissolves again in water and the particles separate more easily than without any redispersing additives [160]. As the PEG dissolves an osmotic pressure arises that draws water into the agglomerates. Stresses as high as 0.6 MPa can occur. According to the experiments by Moon the redispersion was improved from 12.8 to 39.1% by adding PEG 400 for the slurries that were used [160].

However, high molecular weight PEG shows lower solubility in water. With their long chains they hold particles together and due to the low solubility prevent an easy redispersion of the particles in water [160]. Ideally the PEG amount is adjusted so that the excess pressure is slightly higher than the cohesive strength of the powder bed [159]. It is crucial to keep in mind that some PEG is lost if the powder bed is exposed to higher temperatures due to volatilization [140]. This loss of PEG can be reduced by adding butylated hydroxytoluene [159].

Especially for complex parts including channels or undercuts an easy removal of the organic additives is necessary. Combinations of vibration and air blowing are suggested as well as immersion of the printed part in carbonated water and then drawing vacuum so that the escaping CO_2 bubbles drag away any loose powder [164].

2.3. Comparison of powder-based and slurry-based layer deposition

As shown in this work there are plenty of parameters for slurry-based deposition as well as for powder-based layer deposition influencing the final powder bed density. A comparison of green and final powder bed density can be found in Du's review [104]. Due to the many factors on

the density a general quantitative comparison between slurry- and powder-based layer deposition is not possible. However, practical differences can be described qualitatively. This chapter provides such a general overview and contrasts the two deposition methods.

Table 1 provides an overview of the compared points which are explained further in the text.

As visible Table 1 the use of slurries instead of powders to spread a powder layer entails extra work: preparation of a slurry, handling of potential layer cracking, an extra drying step and a more time-consuming depowdering step. This effort can be justified by the advantages offered by the slurry-based process. For the slurry-based process there are no special powder requirements like particle size and flowability as in the powder-based process. Very small powders, even in the submicron range, can be used which leads to higher feature definition and enhanced sinterability [165]. Density of the final part is not only improved by usage of fine powders but also due to the high densities of the green parts achieved by utilizing the slurry instead of powder deposition and thereby allowing free arrangement of the particles to form a dense packing [5,166]. The general trend for higher green densities for the slurry-based process is also demonstrated in the review from Du when comparing the densities achieved for different deposition methods and powder treatments [104]. Another benefit of the high green density is that no sinking or displacement occurs and thus supporting structures are no longer required. SiSiC was printed with the slurry-based binder jetting just to take advantage of the high density but not due to the necessity of using fine powder [167]. Several companies have already shown that the powder-based route is working, too, for SiSiC [168–171]. However, the slurry-based process offers the chance of reducing post-processing steps by printing parts with a high green density and thereby achieving better final part properties. Due to the possibility of using finer powders in slurry deposition also the layer thickness can be smaller than in the powder-based process and therefore the resolution can be higher and stair case effect is reduced [5].

Moreover, some of the printing problems that can occur in powder-based binder jetting can be avoided by using slurry-based processes. As the powder-based powder bed is not completely dense some densification can occur when load for example by printing binder is applied. The powder bed can compress at some areas causing the layer to be slightly displaced. This can have a significant effect on final part quality as Lee observed some downward displacement of parts [54]. Higher cohesive forces between the particles will lead to a less significant displacement. Cohesive forces are usually higher for slurry-based powder beds than for powder-based powder beds. Generally, moisture or high packing density can increase the cohesive forces [88,172]. The powder-based process is also more sensitive to moisture content in the build area as this can for example affect the flowability [173] or wettability [174] of powders.

Another effect only reported for the powder-based process is the so-called balling. xThe printing pattern is then destroyed [69,130]. This can only occur if binder droplet impacting the surface is faster than binder infiltration [175]. Balling can be reduced by improving wetting e.g. by coating powders with wetting agents [69] or changing surface tension of the binder or viscosity [176]. Balling is much more common for finer powders as these are more mobile in the liquid binder/powder mixture caused by the binder drop on the surface [69]. Balling can also happen in laser melting of metals and ceramics and is more likely in powder-based processes [177].

Particle rearrangement due to capillary forces caused by insufficient drying of binder of the previous layer is less likely than in powder-based process [132]. Not completely dried binder can cause tearing and shifting while depositing the next layer in the powder-based process. The moisture of the not yet dry binder causes agglomeration of the powder in front of the spreading device. These agglomerates can lead to bumpy surfaces or shifting of layers [75].

The ballistic ejection [178] caused by binder droplets impacting on the surface of the powder bed is also avoided or significantly decreased using slurry instead of powder deposition. Binder droplets impacting the powder surface with a speed of about 10 m/s can eject or displace particles of the powder bed. As the inter-particle forces in powder beds formed by slurry deposition is higher than for the ones made by powder deposition, no defects related to ballistic ejection were reported yet [75].

So far, no reports of curling, seen as upward bending of the component due to inhomogeneous binder shrinkage, for slurry-based processes have been found whereas curling is a known effect in powder-based binder jetting [179].

Another challenge occurring in powder-based binder jetting is warping due to different drying speeds [133].

3. Conclusion

A variety of powder deposition systems are available that can be used in binder jetting or powder bed fusion. First it is important to decide between a slurry or powder feedstock. A slurry feedstock should be used if fine particles have to be utilized or if high densities without further treatments like part infiltration are needed. If such demands are not required powder-based layer deposition is often the better choice due to the higher printing speed and less difficult depowdering. For both process variants different deposition devices exist and spreading parameters have to be adapted to the powder used.

Both processes allow successful production of technical ceramics and show continuously new material in development. For example alumina [140,162,165,180,181], silicon nitride [164,165,178], silica [182] and more recently silicon carbide [59,167] and porcelain [183] have been produced by slurry-based process. Examples for ceramics

Table 1
Comparison between powder-based and slurry-based layer deposition.

Process Step	Powder-based layer deposition	Slurry-based layer deposition
Powder deposition		
Feedstock requirements	Flowable powder necessary	Slurry preparation necessary, no special powder requirements
Deposition speed	Fast	Slow due to necessary additional drying
Challenges during deposition	Inhomogeneities, holes	Inhomogeneities, cracking
Surface quality	Dependent on powder source	Usually better than in powder-based process
Layer Thickness	Medium –> high	Small –> medium
Powder bed density	Low	High
Depowdering		
Complex geometries	Easy	Slow process (redispersion)
Channels	Possible	Difficult or impossible to clean from powder

made by powder-based process are tricalcium phosphate [88], alumina [184], silicon carbide [185,186] or porcelain [109]. A more complete overview of materials already used in binder jetting and laser sintering can be found in other review works [5,26,100,104,187]. Nevertheless, densities and therefore often mechanical properties are generally lower for powder-bed process [51]. These instances show that the selection of the desired method is dependent on the required final parts properties.

Declaration of competing interest

The authors declare that they have no known competing financial interests or personal relationships that could have appeared to influence the work reported in this paper.

References

[1] S. Jang, S. Park, C.-J. Bae, Development of ceramic additive manufacturing: process and materials technology, Biomed. Eng. Lett. 10 (2020) 493–503, https://doi.org/10.1007/s13534-020-00175-4.
[2] ASTM, Standard Terminology for Additive Manufacturing Technologies, 2015.
[3] Z. Chen, Z. Li, J. Li, C. Liu, C. Lao, Y. Fu, C. Liu, Y. Li, P. Wang, Y. He, 3D printing of ceramics: a review, J. Eur. Ceram. Soc. 39 (2019) 661–687, https://doi.org/10.1016/j.jeurceramsoc.2018.11.013.
[4] A. Zocca, P. Colombo, C.M. Gomes, J. Günster, Additive manufacturing of ceramics: issues, potentialities, and opportunities, J. Am. Ceram. Soc. 98 (2015) 1983–2001, https://doi.org/10.1111/jace.13700.
[5] Y. Lakhdar, C. Tuck, J. Binner, A. Terry, R. Goodridge, Additive manufacturing of advanced ceramic materials, Prog. Mater. Sci. 116 (2021), 100736, https://doi.org/10.1016/j.pmatsci.2020.100736.
[6] W. Kollenberg, Additive Fertigung keramischer Komponenten: Grundlagen und Anwendung, first ed., 2020.
[7] I. Gibson, D.W. Rosen, B. Stucker, Additive Manufacturing Technologies: Rapid Prototyping to Direct Digital Manufacturing, Springer Science+Business Media LLC, Boston, MA, 2010.
[8] H. Wu, W. Liu, R. He, Z. Wu, Q. Jiang, X. Song, Y. Chen, L. Cheng, S. Wu, Fabrication of dense zirconia-toughened alumina ceramics through a stereolithography-based additive manufacturing, Ceram. Int. 43 (2017) 968–972, https://doi.org/10.1016/j.ceramint.2016.10.027.
[9] C. Weller, R. Kleer, F.T. Piller, Economic implications of 3D printing: market structure models in light of additive manufacturing revisited, Int. J. Prod. Econ. 164 (2015) 43–56, https://doi.org/10.1016/j.ijpe.2015.02.020.
[10] T. Rayna, L. Striukova, From rapid prototyping to home fabrication: how 3D printing is changing business model innovation, Technol. Forecast. Soc. Change 102 (2016) 214–224, https://doi.org/10.1016/j.techfore.2015.07.023.
[11] H. Lipson, M. Kurman, Fabricated: the New World of 3D Printing; the Promise and Peril of a Machine that Can Make (Almost) Anything, J. Wiley & Sons, Indianapolis, Ind, 2013.
[12] I.D. Marinescu (Ed.), Handbook of Advanced Ceramics Machining, CRC Press, Boca Raton, Fla, 2007.
[13] W. Li, A. Martin, B. Kroehler, A. Henderson, T. Huang, J.L. Watts, G. Hilmas, M.-C. Leu (Eds.), Fabricating Functionally Graded Materials by Ceramic On-Demand Extrusion with Dynamic Mixing, 2018.
[14] Ina Cheibas, Popovich Vera, Bee Rich, Mathilde Laot, Sarah Rodriguez Castillo, Additive Manufacturing of Functionally Graded Materials with In-SITU Resources, figshare, 2021.
[15] A. Dawood, B. Marti Marti, V. Sauret-Jackson, A. Darwood, 3D printing in dentistry, Br. Dent. J. 219 (2015) 521–529, https://doi.org/10.1038/sj.bdj.2015.914.
[16] N. Guo, M.C. Leu, Additive manufacturing: technology, applications and research needs, Front. Mech. Eng. 8 (2013) 215–243, https://doi.org/10.1007/s11465-013-0248-8.
[17] Sinto, Additive Manufacturing of Ceramics for Biomedical Applications, 2021. https://sintoamerica.com/additive-manufacturing-of-ceramics-for-biomedical-applications/.
[18] Y. Wen, S. Xun, M. Haoye, S. Baichuan, C. Peng, L. Xuejian, Z. Kaihong, Y. Xuan, P. Jiang, L. Shibi, 3D printed porous ceramic scaffolds for bone tissue engineering: a review, Biomater. Sci. 5 (2017) 1690–1698, https://doi.org/10.1039/c7bm00315c.
[19] A.G. Voxeljet. https://www.voxeljet.de/, 2021. (Accessed 8 January 2020) accessed.
[20] C.R. Deckard, US 4,863,538, 1986.
[21] J. Deckers, J. Vleugels, J. Kruth, Additive manufacturing of ceramics: a review, J. Ceram. Sci. Technol. 5 (2014) 245–260.
[22] G.N. Levy, R. Schindel, J.P. Kruth, Rapid Manufacturing and rapid tooling with layer manufacturing (LM) technologies, state of the art and future perspectives, CIRP Ann. 52 (2003) 589–609, https://doi.org/10.1016/S0007-8506(07)60206-6.
[23] A.S. Klimov, I.Y. Bakeev, E.S. Dvilis, E.M. Oks, A.A. Zenin, Electron beam sintering of ceramics for additive manufacturing, Vacuum 169 (2019), 108933, https://doi.org/10.1016/j.vacuum.2019.108933.
[24] T.R. Mahale, Electron Beam Melting of Advanced Materials and Structures, Mass Customization, mass personalization, 2009.
[25] J.-P. Kruth, P. Mercelis, J. van Vaerenbergh, L. Froyen, M. Rombouts, Binding mechanisms in selective laser sintering and selective laser melting, Rapid Prototyp. J. 11 (2005) 26–36, https://doi.org/10.1108/13552540510573365.
[26] S.L. Sing, W.Y. Yeong, F.E. Wiria, B.Y. Tay, Z. Zhao, L. Zhao, Z. Tian, S. Yang, Direct selective laser sintering and melting of ceramics: a review, RPJ 23 (2017) 611–623, https://doi.org/10.1108/RPJ-11-2015-0178.
[27] H. Yves-Christian, W. Jan, M. Wilhelm, W. Konrad, P. Reinhart, Net shaped high performance oxide ceramic parts by selective laser melting, Phys. Procedia 5 (2010) 587–594, https://doi.org/10.1016/j.phpro.2010.08.086.
[28] B. Qian, Z. Shen, Laser sintering of ceramics, J. Asian Ceram. Soc. 1 (2013) 315–321, https://doi.org/10.1016/j.jascer.2013.08.004.
[29] E. Juste, F. Petit, V. Lardot, F. Cambier, Shaping of ceramic parts by selective laser melting of powder bed, J. Mater. Res. 29 (2014) 2086–2094, https://doi.org/10.1557/jmr.2014.127.
[30] J.F. Li, L. Li, F.H. Stott, Comparison of volumetric and surface heating sources in the modeling of laser melting of ceramic materials, Int. J. Heat Mass Tran. 47 (2004) 1159–1174, https://doi.org/10.1016/j.ijheatmasstransfer.2003.10.002.
[31] P. Mercelis, J.-P. Kruth, Residual stresses in selective laser sintering and selective laser melting, Rapid Prototyp. J. 12 (2006) 254–265, https://doi.org/10.1108/13552540610707013.
[32] Z.H. Liu, J.J. Nolte, J.I. Packard, G. Hilmas, F. Dogan, M.C. Leu, Selective laser sintering of high-density alumina ceramic parts, in: S. Hinduja, K.-C. Fan (Eds.), Proceedings of the 35th International MATADOR Conference: Formerly the International Machine Tool Design and Research Conference, Springer, London, 2007, pp. 351–354.
[33] H.-H. Tang, M.-L. Chiu, H.-C. Yen, Slurry-based selective laser sintering of polymer-coated ceramic powders to fabricate high strength alumina parts, J. Eur. Ceram. Soc. 31 (2011) 1383–1388, https://doi.org/10.1016/j.jeurceramsoc.2011.02.020.
[34] W. Wang, S. Ma, J.Y.H. Fuh, L. Lu, Y. Liu, Processing and characterization of laser-sintered Al2O3/ZrO2/SiO2, Int. J. Adv. Manuf. Technol. 68 (2013) 2565–2569, https://doi.org/10.1007/s00170-013-4863-7.
[35] I. Lee, Influence of heat treatment upon SLS processed composites fabricated with alumina and monoclinic HBO2, J. Mater. Sci. Lett. 21 (2002) 209–212, https://doi.org/10.1023/A:1014756724160.
[36] J.-J. Kim, Kim, Byung-Ki, Song, Byung-Moo, Doh-Yeon Kim, D.N. Yoon, Effect of sintering atmosphere on isolated pores during the liquid-phase sintering of MgO-CaMgSiO4, J. Am. Ceram. Soc. 70 (1987) 734–737, https://doi.org/10.1111/j.1151-2916.1987.tb04872.x.
[37] F.-H. Liu, Y.-S. Liao, Fabrication of inner complex ceramic parts by selective laser gelling, J. Eur. Ceram. Soc. 30 (2010) 3283–3289, https://doi.org/10.1016/j.jeurceramsoc.2010.08.001.
[38] M. Geiger (Ed.), Laser Assisted Net Shape Engineering 2: Proceedings of the 30th International CIRP Seminar on Manufacturing Systems - LANE '97, Meisenbach, Bamberg, 1997. Erlangen, September 23 - 26, 1997.
[39] T.B. Sercombe, G.B. Schaffer, Rapid manufacturing of aluminum components, Science 301 (2003) 1225–1227.
[40] J.-Y. Lee, J. An, C.K. Chua, Fundamentals and applications of 3D printing for novel materials, Appl. Mater. Today 7 (2017) 120–133, https://doi.org/10.1016/j.apmt.2017.02.004.
[41] B. Stevinson, D.L. Bourell, J.J.J. Beaman, Dimensional stability during post-processing of selective laser sintered ceramic preforms, Virtual Phys. Prototyp. 1 (2006) 209–216, https://doi.org/10.1080/17452750601107003.
[42] D.M. Gureev, R.V. Ruzhechko, I.V. Shishkovskii, Selective laser sintering of PZT ceramic powders, Tech. Phys. Lett. 26 (2000) 262–264, https://doi.org/10.1134/1.1262811.
[43] F. Chen, J.-M. Wu, H.-Q. Wu, Y. Chen, C.-H. Li, Y.-S. Shi, Microstructure and mechanical properties of 3Y-TZP dental ceramics fabricated by selective laser sintering combined with cold isostatic pressing, Int. J. Lightweight Mater. Manufact. 1 (2018) 239–245, https://doi.org/10.1016/j.ijlmm.2018.09.002.
[44] Y. Shi, Additive manufacturing of zirconia parts via selective laser sintering combined with cold isostatic pressing, JME (J. Med. Ethics) 50 (2014) 118, https://doi.org/10.3901/JME.2014.21.118.
[45] K. Liu, C.H. Li, W.T. He, Y.S. Shi, J. Liu, Investigation into indirect selective laser sintering alumina ceramic parts combined with cold isostatic pressing, AMM 217–219 (2012) 2217–2221. https://doi.org/10.4028/www.scientific.net/AMM.217-219.2217.
[46] A. Mussatto, R. Groarke, A. O'Neill, M.A. Obeidi, Y. Delaure, D. Brabazon, Influences of powder morphology and spreading parameters on the powder bed topography uniformity in powder bed fusion metal additive manufacturing, Add. Manufact. 38 (2021), 101807, https://doi.org/10.1016/j.addma.2020.101807.
[47] R. Kumar, A.K. Jana, S.R. Gopireddy, C.M. Patel, Effect of horizontal vibrations on mass flow rate and segregation during hopper discharge: discrete element method approach, Sādhanā 45 (2020), https://doi.org/10.1007/s12046-020-1300-0.
[48] R. Morgan, C.J. Sutcliffe, W. O'Neill, Experimental investigation of nanosecond pulsed Nd:YAG laser re-melted pre-placed powder beds, Rapid Prototyp. J. 7 (2001) 159–172, https://doi.org/10.1108/13552540110395565.
[49] E. Sachs, S. Haggerty, J. Michael, P.A. Williams, US 5204055-A, 1993.
[50] B.R. Utela, D. Storti, R.L. Anderson, M. Ganter, Development process for custom three-dimensional printing (3DP) material systems, J. Manuf. Sci. Eng. 132 (2010), 011008, https://doi.org/10.1115/1.4000713.
[51] A. Mostafaei, A.M. Elliott, J.E. Barnes, F. Li, W. Tan, C.L. Cramer, P. Nandwana, M. Chmielus, Binder jet 3D printing—process parameters, materials, properties,

modeling, and challenges, Prog. Mater. Sci. (2020), 100707, https://doi.org/10.1016/j.pmatsci.2020.100707.
[52] ExOne Company, The ExOne Triple Act.
[53] E. Sachs, M. Cima, P. Williams, D. Brancazio, J. Cornie, Three dimensional printing: rapid tooling and prototypes directly from a CAD model, J. Eng. Indust. 114 (1992) 481–488, https://doi.org/10.1115/1.2900701.
[54] S.-J.J. Lee, E. Sachs, M. Cima, Powder layer position accuracy in powder-based rapid prototyping, in: Conference Proceedings International Solid Freeform Fabrication Symposium, 1993.
[55] G.A. Fielding, A. Bandyopadhyay, S. Bose, Effects of silica and zinc oxide doping on mechanical and biological properties of 3D printed tricalcium phosphate tissue engineering scaffolds, Dent. Mater. 28 (2012) 113–122, https://doi.org/10.1016/j.dental.2011.09.010.
[56] W. Zhang, R. Melcher, N. Travitzky, R.K. Bordia, P. Greil, Three-dimensional printing of complex-shaped alumina/glass composites, Adv. Eng. Mater. (2009), https://doi.org/10.1002/adem.200900213. NA-NA.
[57] R. Melcher, S. Martins, N. Travitzky, P. Greil, Fabrication of Al2O3-based composites by indirect 3D-printing, Mater. Lett. 60 (2006) 572–575, https://doi.org/10.1016/j.matlet.2005.09.059.
[58] Z. Fu, L. Schlier, N. Travitzky, P. Greil, Three-dimensional printing of SiSiC lattice truss structures, Mater. Sci. Eng. A 560 (2013) 851–856, https://doi.org/10.1016/j.msea.2012.09.107.
[59] J. Moon, A.C. Caballero, L. Hozer, Y.-M. Chiang, M.J. Cima, Fabrication of functionally graded reaction infiltrated SiC–Si composite by three-dimensional printing (3DP™) process, Mater. Sci. Eng. A 298 (2001) 110–119, https://doi.org/10.1016/S0921-5093(00)01282-X.
[60] J. Yoo, M. Cima, S. Khanuja, E. Sachs, Structural Ceramic Components by 3D Printing, 1993.
[61] W. Sun, D.J. Dcosta, F. Lin, T. El-Raghy, Freeform fabrication of Ti3SiC2 powder-based structures: Part I—integrated fabrication process, J. Mater. Process. Technol. 127 (2002) 343–351, https://doi.org/10.1016/S0924-0136(02)00284-4.
[62] M.N. Rahaman, Kinetics and mechanisms of densification, in: Z.Z. Fang (Ed.), Sintering of Advanced Materials: Fundamentals and Processes, Woodhead Pub, Oxford, Philadelphia, PA, 2010, pp. 33–64.
[63] P.L. Mangonon, The Principles of Materials Selection for Engineering Design, Prentice Hall, Upper Saddle River, NJ, 1999.
[64] F.R.N. Nabarro, Steady-state diffusional creep, Phil. Mag. 16 (1967) 231–237, https://doi.org/10.1080/14786436708229736.
[65] J.S. Reed, Principles of Ceramics Processing, second., Wiley, New York, 1995.
[66] D. Schulze, Powders and Bulk Solids: Behavior, Characterization, Storage and Flow, Springer, Berlin, 2008.
[67] J.F. Bredt, Binder Stability and Powder/binder Interaction in Three Dimensional Printing, Doctoral Thesis, 1995.
[68] K.J. Seluga, Three Dimensional Printing by Vector Printing of Fine Metal Powders, Disseratation, 2001.
[69] P.R. Baker, Three Dimensional Printing with Fine Metal Powders, Dissertation, 1997.
[70] S. Yang, J.R.G. Evans, Metering and dispensing of powder; the quest for new solid freeforming techniques, Powder Technol. 178 (2007) 56–72, https://doi.org/10.1016/j.powtec.2007.04.004.
[71] C. Meier, R. Weissbach, J. Weinberg, W.A. Wall, A.J. Hart, Critical influences of particle size and adhesion on the powder layer uniformity in metal additive manufacturing, J. Mater. Process. Technol. 266 (2019) 484–501, https://doi.org/10.1016/j.jmatprotec.2018.10.037.
[72] B. Nagarajan, Z. Hu, X. Song, W. Zhai, J. Wei, Development of micro selective laser melting: the state of the art and future perspectives, Engineering 5 (2019) 702–720, https://doi.org/10.1016/j.eng.2019.07.002.
[73] A.T. Sutton, C.S. Kriewall, M. Leu, J. Newkirk, Powders for Additive Manufacturing Processes: Characterization Techniques and Effects on Part Properties, 2016.
[74] J.G. Berryman, Random close packing of hard spheres and disks, Phys. Rev. A 27 (1983) 1053–1061, https://doi.org/10.1103/PhysRevA.27.1053.
[75] S.J. Gregorski, High Green Density Metal Parts by Vibrational Compaction of Dry Powder in Three Dimensional Printing Process, Thesis, 1996.
[76] R.M. German, Powder Metallurgy Science, second., Metal Powder Industries Federation, Princeton, N.J, 1994.
[77] N.P. Karapatis, G. Egger, P.E. Gygax, R. Glardon, Optimization of Powder Layer Density in Selective Laser Sintering, The University of Texas at Austin, 1999.
[78] C.C. Furnas, Grading aggregates - I. - mathematical relations for beds of broken solids of maximum density, Ind. Eng. Chem. 23 (1931) 1052–1058, https://doi.org/10.1021/ie50261a017.
[79] W. Man, A. Donev, F.H. Stillinger, M.T. Sullivan, W.B. Russel, D. Heeger, S. Inati, S. Torquato, P.M. Chaikin, Experiments on random packings of ellipsoids, Phys. Rev. Lett. 94 (2005) 198001, https://doi.org/10.1103/PhysRevLett.94.198001.
[80] X. Chateau, Particle packing and the rheology of concrete, in: Understanding the Rheology of Concrete, Elsevier, 2012, pp. 117–143.
[81] S. Vock, B. Klöden, A. Kirchner, T. Weißgärber, B. Kieback, Powders for powder bed fusion: a review, Prog Addit Manuf 4 (2019) 383–397, https://doi.org/10.1007/s40964-019-00078-6.
[82] J. Zheng, P.F. Johnson, J.S. Reed, Improved equation of the continuous particle size distribution for dense packing, J. Am. Ceram. Soc. 73 (1990) 1392–1398, https://doi.org/10.1111/j.1151-2916.1990.tb05210.x.
[83] C. Herring, Effect of change of scale on sintering phenomena, J. Appl. Phys. 21 (1950) 301–303, https://doi.org/10.1063/1.1699658.
[84] S.-J.L. Kang, Y.-I. Jung, Sintering kinetics at final stage sintering: model calculation and map construction, Acta Mater. 52 (2004) 4573–4578, https://doi.org/10.1016/j.actamat.2004.06.015.
[85] J. Zhao, M.P. Harmer, Sintering kinetics for a model final-stage microstructure: a study of AI 2 O 3, Phil. Mag. Lett. 63 (1991) 7–14, https://doi.org/10.1080/09500839108206594.
[86] E.M. Sachs, M.J. Cima, M.A. Caradonna, J. Grau, J.G. Serdy, P.C. Saxton, S. A. Uhland, J. Moon US 6 (224) (2003) 596.
[87] A. Budding, T.H.J. Vaneker, New strategies for powder compaction in powder-based rapid prototyping techniques, Procedia CIRP 6 (2013) 527–532, https://doi.org/10.1016/j.procir.2013.03.100.
[88] A. Butscher, M. Bohner, S. Hofmann, L. Gauckler, R. Müller, Structural and material approaches to bone tissue engineering in powder-based three-dimensional printing, Acta Biomater. 7 (2011) 907–920, https://doi.org/10.1016/j.actbio.2010.09.039.
[89] H. Miyanaji, L. Yang (Eds.), Equilibrium Saturation in Binder Jetting Additive Manufacturing Processes: Theoretical Model vs, Experimental Observations, 2016.
[90] ISO International Standards, Surface Active Agents - Powders and Granules - Measurement of the Angle of Repose, 1977. https://www.iso.org/standard/10196.html. (Accessed 21 January 2021). accessed.
[91] F. Amado, M. Schmid, G. Levy, K. Wegener, Advances in SLS Powder Characterization, 2011.
[92] H. Fayazfar, M. Salarian, A. Rogalsky, D. Sarker, P. Russo, V. Paserin, E. Toyserkani, A critical review of powder-based additive manufacturing of ferrous alloys: process parameters, microstructure and mechanical properties, Mater. Des. 144 (2018) 98–128, https://doi.org/10.1016/j.matdes.2018.02.018.
[93] R.L. Plaut, C. Herrera, D.M. Escriba, P.R. Rios, A.F. Padilha, A Short review on wrought austenitic stainless steels at high temperatures: processing, microstructure, properties and performance, Mat. Res. 10 (2007) 453–460, https://doi.org/10.1590/S1516-14392007000400021.
[94] ASTM, Standard Test Methods for Flow Rate of Metal Powders Using the Hall Flowmeter Funnel.
[95] R. Freeman, Measuring the flow properties of consolidated, conditioned and aerated powders — a comparative study using a powder rheometer and a rotational shear cell, Powder Technol. 174 (2007) 25–33, https://doi.org/10.1016/j.powtec.2006.10.016.
[96] J.K. Beddow, Professor dr. Henry H. Hausner, 1900-1995, part. Part, Syst. Char. 12 (1995) 213, https://doi.org/10.1002/ppsc.19950120411.
[97] G.G.Z. Zhang, L.X. Yu, R.V. Mantri, Y. Qiu, Y. Chen (Eds.), Developing Solid Oral Dosage Forms: Pharmaceutical Theory & Practice, Academic Press, Amsterdam, 2017.
[98] A. Santomaso, P. Lazzaro, P. Canu, Powder flowability and density ratios: the impact of granules packing, Chem. Eng. Sci. 58 (2003) 2857–2874, https://doi.org/10.1016/S0009-2509(03)00137-4.
[99] M. Krantz, H. Zhang, J. Zhu, Characterization of powder flow: static and dynamic testing, Powder Technol. 194 (2009) 239–245, https://doi.org/10.1016/j.powtec.2009.05.001.
[100] D. Grossin, A. Montón, P. Navarrete-Segado, E. Özmen, G. Urruth, F. Maury, D. Maury, C. Frances, M. Tourbin, P. Lenormand, G. Bertrand, A review of additive manufacturing of ceramics by powder bed selective laser processing (sintering/melting): calcium phosphate, silicon carbide, zirconia, alumina, and their composites, Open Ceram. 5 (2021), 100073, https://doi.org/10.1016/j.oceram.2021.100073.
[101] H. Chen, Q. Wei, S. Wen, Z. Li, Y. Shi, Flow behavior of powder particles in layering process of selective laser melting: numerical modeling and experimental verification based on discrete element method, Int. J. Mach. Tool Manufact. 123 (2017) 146–159, https://doi.org/10.1016/j.ijmachtools.2017.08.004.
[102] A. Crouter, L. Briens, The effect of moisture on the flowability of pharmaceutical excipients, AAPS PharmSciTech (2014) 65–74, https://doi.org/10.1208/s12249-013-0036-0.
[103] A. Rescaglio, J. Schockmel, N. Vandewalle, G. Lumay, Combined effect of moisture and electrostatic charges on powder flow, EPJ Web Conf. 140 (2017), 13009, https://doi.org/10.1051/epjconf/201714013009.
[104] W. Du, X. Ren, Z. Pei, C. Ma, Ceramic binder jetting additive manufacturing: a literature review on density, J. Manuf. Sci. Eng. 142 (2020), 040801, https://doi.org/10.1115/1.4046248.
[105] J.H. Tan, W.L.E. Wong, K.W. Dalgarno, An overview of powder granulometry on feedstock and part performance in the selective laser melting process, Add. Manufact. 18 (2017) 228–255, https://doi.org/10.1016/j.addma.2017.10.011.
[106] A. Spillmann, A. Sonnenfeld, P.R. von Rohr, Flowability modification of lactose powder by plasma enhanced chemical vapor deposition, Plasma Process. Polym. 4 (2007) S16–S20, https://doi.org/10.1002/ppap.200730202.
[107] D. Sofia, R. Chirone, P. Lettieri, D. Barletta, M. Poletto, Selective laser sintering of ceramic powders with bimodal particle size distribution, Chem. Eng. Res. Des. 136 (2018) 536–547, https://doi.org/10.1016/j.cherd.2018.06.008.
[108] S. Dadbakhsh, L. Verbelen, T. Vandeputte, D. Strobbe, P. van Puyvelde, J.-P. Kruth, Effect of powder size and shape on the SLS processability and mechanical properties of a TPU elastomer, Phys. Procedia 83 (2016) 971–980, https://doi.org/10.1016/j.phpro.2016.08.102.
[109] H. Miyanaji, S. Zhang, A. Lassell, A. Zandinejad, L. Yang, Process development of porcelain ceramic material with binder jetting process for dental applications, JOM 68 (2016) 831–841, https://doi.org/10.1007/s11837-015-1771-3.
[110] H. Miyanaji, M. Orth, J.M. Akbar, L. Yang, Process development for green part printing using binder jetting additive manufacturing, Front. Mech. Eng. 13 (2018) 504–512, https://doi.org/10.1007/s11465-018-0508-8.

[111] Y. Shanjani, E. Toyserkani, Material Spreading and Compaction In Powder-based Solid Freeform Fabrication Methods Mathematical Modeling, 2008.
[112] Y.M. Fouda, A.E. Bayly, A DEM study of powder spreading in additive layer manufacturing, Granul. Matter 22 (2020), https://doi.org/10.1007/s10035-019-0971-x.
[113] T. Davidson, A.T. Hernandez, J. Kinsley, J. Sanchez, (Z Corporation) US 7,828,022 B2, 2010.
[114] H. Perret, B. Graf, U.C. Sagmeister US-6672343-B1.
[115] D. Brunermer, US 8,568,124 B2, 2011.
[116] R. Hochsmann, I. Ederer EP0882568B8, 1998.
[117] E. Sachs, US6,036,777, 2000.
[118] J. Guo, A. Roberts, M. Jones, Some theoretical consideration of stress states at the hopper feeder interface, in: The 13th International Conference on Bulk Materials Storage, Handling and Transportation, ICBMH, 2019, pp. 870–878.
[119] P.E. Rogren, US2015314530A1, 2017.
[120] S.A. Aerosint, Dual-metal L-PBF Printer. https://aerosint.com/dual-metal-lpbf/. (Accessed 30 July 2021) accessed.
[121] M. Cima, E. Sachs, T. Fan, J.F. Bredt, S.P. Michaels, S. Khanuja, A. Lauder, S.-J. J. Lee, D. Brancazio, A. Curodeau, H. Tuerck, US-5,387,380, 1995.
[122] S. Tochimoto, N. Kubo, US-6799959-B1, 2004.
[123] S. Haeri, Y. Wang, O. Ghita, J. Sun, Discrete element simulation and experimental study of powder spreading process in additive manufacturing, Powder Technol. 306 (2017) 45–54, https://doi.org/10.1016/j.powtec.2016.11.002.
[124] S. Haeri, Optimisation of blade type spreaders for powder bed preparation in Additive Manufacturing using DEM simulations, Powder Technol. 321 (2017) 94–104, https://doi.org/10.1016/j.powtec.2017.08.011.
[125] S. Beitz, R. Uerlich, T. Bokelmann, A. Diener, T. Vietor, A. Kwade, Influence of Powder Deposition on Powder Bed and Specimen Properties, Materials (Basel), vol. 12, 2019, https://doi.org/10.3390/ma12020297.
[126] S. Spath, H. Seitz, Influence of grain size and grain-size distribution on workability of granules with 3D printing, Int. J. Adv. Manuf. Technol. 70 (2014) 135–144, https://doi.org/10.1007/s00170-013-5210-8.
[127] T. Niino, K. Sato, Effect of Powder Compaction in Plastic Laser Sintering Fabrication, 2009.
[128] D. Drummer, M. Drexler, F. Kühnlein, Effects on the density distribution of SLS-parts, Phys. Procedia 39 (2012) 500–508, https://doi.org/10.1016/j.phpro.2012.10.066.
[129] S. Haeri, Enhancement of the spreading process in additive manufacturing through the spreader optimisation, in: International Conference on Particle-Based Methods - Fundamentals and Applications.
[130] S. Cao, Y. Qiu, X.-F. Wei, H.-H. Zhang, Experimental and theoretical investigation on ultra-thin powder layering in three dimensional printing (3DP) by a novel double-smoothing mechanism, J. Mater. Process. Technol. 220 (2015) 231–242, https://doi.org/10.1016/j.jmatprotec.2015.01.016.
[131] S.E. Perrin, Control of Thin Layer Powder Packing Density Effects of Applied Vibration, Thesis B.Sc., 1991.
[132] E. Sachs, US-6036777-A, 2000.
[133] S.S. Khanjua, Origin and Control of Anisotropy in Three Dimensional Printing of Structural Ceramics, Thesis (Ph. D.), 1996.
[134] T.D. Szucs, D. Brabazon, Analysis of the Effects of 3DP Parameters on Part Feature Dimensional Accuracy, The University of Texas at Austin, 2007.
[135] H. Haferkamp, A. Ostendorf, H. Becker, S. Czerner, P. Stippler, Combination of Yb:YAG-disc laser and roll-based powder deposition for the micro-laser sintering, J. Mater. Process. Technol. 149 (2004) 623–626, https://doi.org/10.1016/j.jmatprotec.2004.02.056.
[136] P. Regenfuß, R. Ebert, H. Exner, Laser micro sintering – a versatile instrument for the generation of microparts, LTJ 4 (2007) 26–31, https://doi.org/10.1002/latj.200790139.
[137] A. Zocca, C.M. Gomes, T. Mühler, J. Günster, Powder-bed stabilization for powder-based additive manufacturing, Adv. Mech. Eng. 6 (2014), 491581, https://doi.org/10.1155/2014/491581.
[138] J. Günster, A. Zocca, C.M. Gomes, T. Mühler, US9533452B2, 2017.
[139] F. Chinellato, J. Wilbig, D. Al-Sabbagh, P. Colombo, J. Günster, Gas flow assisted powder deposition for enhanced flowability of fine powders: 3D printing of α-tricalcium phosphate, Open Ceram. 1 (2020), 100003, https://doi.org/10.1016/j.oceram.2020.100003.
[140] J.E. Grau, Fabrication of Engineered Ceramic Components by the Slurry-Based Three Dimensional Printing Process, 1998.
[141] T. Mühler, C.M. Gomes, J. Heinrich, J. Günster, Slurry-based additive manufacturing of ceramics, Int. J. Appl. Ceram. Technol. 12 (2015) 18–25, https://doi.org/10.1111/ijac.12113.
[142] X. Tian, J. Günster, J. Melcher, D. Li, J.G. Heinrich, Process parameters analysis of direct laser sintering and post treatment of porcelain components using Taguchi's method, J. Eur. Ceram. Soc. 29 (2009) 1903–1915, https://doi.org/10.1016/j.jeurceramsoc.2008.12.002.
[143] A. Gahler, J.G. Heinrich, J. Günster, Direct laser sintering of Al 2 O 3 ?SiO 2 dental ceramic components by layer-wise slurry deposition, J. Am. Ceram. Soc. 89 (2006) 3076–3080, https://doi.org/10.1111/j.1551-2916.2006.01217.x.
[144] T. Krause, S. Engler, J. Günster, J.G. Heinrich, US20030001313A1, 2004.
[145] J. Günster, C.M. Gomes, EP2714354B1, 2019.
[146] H.C. Yen, Experimental studying on development of slurry-layer casting system for additive manufacturing of ceramics, Int. J. Adv. Manuf. Technol. 77 (2015) 915–925, https://doi.org/10.1007/s00170-014-6534-8.
[147] J. Günster, A. Zocca, J. Lüchentborg, DE102017126274B4, 2019.
[148] J.E. Grau, S.A. Uhland, J. Moon, M.J. Cima, E.M. Sachs, Controlled cracking of multilayer ceramic bodies, J. Am. Ceram. Soc. 82 (1999) 2080–2086, https://doi.org/10.1111/j.1151-2916.1999.tb02044.x.
[149] X. Tian, D. Li, J.G. Heinrich, Rapid prototyping of porcelain products by layer-wise slurry deposition (LSD) and direct laser sintering, Rapid Prototyp. J. 18 (2012) 362–373, https://doi.org/10.1108/13552541211250364.
[150] M. Murray, Cracking in coatings from colloidal dispersions - an industrial perspective. file:///C:/Users/ad899/AppData/Local/Temp/Murray-1.pdf, 2009. (Accessed 24 November 2020) accessed.
[151] R.C. Chiu, T.J. Garino, M.J. Cima, Drying of granular ceramic films: I, effect of processing variables on cracking behavior, J. Am. Ceram. Soc. 76 (1993) 2257–2264, https://doi.org/10.1111/j.1151-2916.1993.tb07762.x.
[152] R.C. Chiu, Drying of Granular Ceramic Films, Doctoral Thesis, 1991.
[153] M.S. Hu, M.D. Thouless, A.G. Evans, The decohesion of thin films from brittle substrates, Acta Metall. 36 (1988) 1301–1307.
[154] K.B. Singh, M.S. Tirumkudulu, Cracking in drying colloidal films, Phys. Rev. Lett. 98 (2007) 218302, https://doi.org/10.1103/PhysRevLett.98.218302.
[155] J.A. Lewis, K.A. Blackman, A.L. Ogden, J.A. Payne, L.F. Francis, Rheological property and stress development during drying of tape-cast ceramic layers, J. Am. Ceram. Soc. 79 (1996) 3225–3234, https://doi.org/10.1111/j.1151-2916.1996.tb08099.x.
[156] G.W. Scherer, Theory of drying, J. Am. Ceram. Soc. 73 (1990) 3–14, https://doi.org/10.1111/j.1151-2916.1990.tb05082.x.
[157] W. Lan, P. Xiao, Constrained drying of an aqueous yttria-stabilized zirconia slurry on a substrate II: binary particle slurry, J. Am. Ceram. Soc. 90 (2007) 2771–2778, https://doi.org/10.1111/j.1551-2916.2007.01839.x.
[158] A. Maskara, D.M. Smith, Agglomeration during the drying of fine silica powders, Part II: the role of particle solubility, J. Am. Ceram. Soc. 80 (1997) 1715–1722, https://doi.org/10.1111/j.1151-2916.1997.tb03044.x.
[159] S.A. Uhland, Fabrication of Advanced Ceramic Components Using Slurry-Based Three Dimensional Printing, Ph.D. Thesis, 2000.
[160] J. Moon, J.E. Grau, M.J. Cima, E.M. Sachs, Slurry chemistry control to produce easily redispersible ceramic powder compacts, J. Am. Ceram. Soc. 83 (2000) 2401–2408, https://doi.org/10.1111/j.1151-2916.2000.tb01568.x.
[161] P.M. Heertjes, W.C. Witvoet, Some aspects of the Wetting of powders, Powder Technol. 3 (1969) 339–343, https://doi.org/10.1016/0032-5910(69)80105-1.
[162] Richard K. Holman, Michael J. Cima, A. Scott, Uhland, emanuel Sachs, spreading and infiltration of inkjet-printed polymer solution droplets on a porous substrate, J. Colloid Interface Sci. 249 (2002) 432–440, https://doi.org/10.1006/jcis.2002.8225.
[163] P. Dayal, G. Tirani (Eds.), Hot Isostatic Pressing: HIP'17, Materials Research Forum LLC, 2019.
[164] E. Sachs, S.P. Micheals, S.M. Allen US5775402A, 1995.
[165] A. Zocca, P. Lima, J. Günster, LSD-based 3D printing of alumina ceramics, J. Ceram. Sci. Tech 8 (2017) 141–148.
[166] J.E. Grau, J. Moon, S. Uhland, M. Cima, E. Sachs, E. Sachs, High green density ceramic components fabricated by the slurry-based 3DP process, Mater. Sci. (1997), https://doi.org/10.15781/T2DV1D80B.
[167] A. Zocca, P. Lima, S. Diener, N. Katsikis, J. Günster, Additive manufacturing of SiSiC by layerwise slurry deposition and binder jetting (LSD-print), J. Eur. Ceram. Soc. 39 (2019) 3527–3533, https://doi.org/10.1016/j.jeurceramsoc.2019.05.009.
[168] Ceramtec, Ceramtec - rocar. https://www.ceramtec-industrial.com/de/werkstoffe/siliciumcarbid/rocar. (Accessed 30 July 2021) accessed.
[169] SGL Carbon GmbH, The 3 Designers - Carboprint, Sicaprint.
[170] Schunk Ingenieurkeramik GmbH, IntrinSiC.
[171] Schunk. https://www.schunk-carbontechnology.com/de/technologien/stories/detailseite/intrinsicr-3d-druck-in-voellig-neuer-dimension. (Accessed 30 July 2021) accessed.
[172] E. Sachs, M. Cima, J. Cornie, D. Brancazio, J. Bredt, A. Curodeau, T. Fan, S. Khanuja, A. Lauder, J. Lee, S. Michaels, Three-dimensional printing: the physics and implications of additive manufacturing, CIRP Ann. 42 (1993) 257–260, https://doi.org/10.1016/S0007-8506(07)62438-X.
[173] V. Karde, C. Ghoroi, Fine powder flow under humid environmental conditions from the perspective of surface energy, Int. J. Pharm. 485 (2015) 192–201, https://doi.org/10.1016/j.ijpharm.2015.03.021.
[174] A. Hodgson, S. Haq, Water adsorption and the wetting of metal surfaces, Surf. Sci. Rep. 64 (2009) 381–451, https://doi.org/10.1016/j.surfrep.2009.07.001.
[175] T. Nguyen, W. Shen, K. Hapgood, Drop penetration time in heterogeneous powder beds, Chem. Eng. Sci. 64 (2009) 5210–5221, https://doi.org/10.1016/j.ces.2009.08.038.
[176] Y. Bai, G. Wagner, C. Williams, Effect of Bimodal Powder Mixture on Powder Packing Density and Sintered Density in Binder Jetting of Metals, 2015.
[177] X. Zhou, X. Liu, D. Zhang, Z. Shen, W. Liu, Balling phenomena in selective laser melted tungsten, J. Mater. Process. Technol. 222 (2015) 33–42, https://doi.org/10.1016/j.jmatprotec.2015.02.032.
[178] T. Fan, Droplet-powder Impact Interaction in Three Dimensional Printing, 1995.
[179] M. Kafara, J. Kemnitzer, H.-H. Westermann, R. Steinhilper, Influence of binder quantity on dimensional accuracy and resilience in 3D-printing, Procedia Manufact. 21 (2018) 638–646, https://doi.org/10.1016/j.promfg.2018.02.166.
[180] S. Uhland, R.K. Holman, M. Cima, E. Sachs, Y. Enokido, New process and materials developments in 3-dimensional printing, 3DP, MRS Proc. 542 (1998) 153.
[181] M.J. Cima, M. Oilveira, H.R. Wang, E. Sachs, R. Holman, Slurry-Based 3DP and Fine Ceramic Components, The University of Texas at Austin, 2001.

[182] H.-R. Wang, M.J. Cima, E.M. Sachs, Three-dimensional printing (3DP™) of gradient-index (GRIN) lenses, in: J.P. Singh, N.P. Bansal (Eds.), Innovative Processing and Synthesis of Ceramics, Glasses, and Composites VI: Proceedings of the Innovative Processing and Synthesis of Ceramics, Glasses, and Composites Symposium Held at the 104th Annual Meeting of the American Ceramic Society, St. Louis, Missouri, American Ceramic Society, Westerville, Ohio, 2002, pp. 189–201. April 28-May 1, 2002.

[183] P. Lima, A. Zocca, W. Acchar, J. Günster, 3D printing of porcelain by layerwise slurry deposition, J. Eur. Ceram. Soc. 38 (2018) 3395–3400, https://doi.org/10.1016/j.jeurceramsoc.2018.03.014.

[184] J.A. Gonzalez, J. Mireles, Y. Lin, R.B. Wicker, Characterization of ceramic components fabricated using binder jetting additive manufacturing technology, Ceram. Int. 42 (2016) 10559–10564, https://doi.org/10.1016/j.ceramint.2016.03.079.

[185] A. Fleisher, D. Zolotaryov, A. Kovalevsky, G. Muller-Kamskii, E. Eshed, M. Kazakin, V.V. Popov, Reaction bonding of silicon carbides by Binder Jet 3D-Printing, phenolic resin binder impregnation and capillary liquid silicon infiltration, Ceram. Int. 45 (2019) 18023–18029, https://doi.org/10.1016/j.ceramint.2019.06.021.

[186] C.L. Cramer, A.M. Elliott, E. Lara-Curzio, A. Flores-Betancourt, M.J. Lance, L. Han, J. Blacker, A.A. Trofimov, H. Wang, E. Cakmak, K. Nawaz, Properties of SiC-Si Made via Binder Jet 3D Printing of SiC Powder, Carbon Addition, and Silicon Melt Infiltration, J American Ceramic Society, 2021, https://doi.org/10.1111/jace.17933.

[187] A. Mostafaei, E. Stevens, J. Ference, D. Schmidt, M. Chmielus, Binder jet printing of partial denture metal framework from metal powder, in: Contributed Papers from MS&T17, MS&T17, 2017, pp. 289–291.